2009:036 CIV

MASTER'S THESIS

Fibre based models for predicting tensile strength of paper

Ann Axelsson

Luleå University of Technology

MSc Programmes in Engineering
Wood Engineering
Department of Skellefteå Campus
Division of Wood Science and Technology

2009:036 CIV - ISSN: 1402-1617 - ISRN: LTU-EX--09/036--SE

Preface

This study was carried out at SCA R&D Centre in Sundsvall, Sweden and the purpose was to enhance the understanding of the connection between the wood fibres and the tensile strength of paper.

I would like to thank everyone that has helped and guided me through the project, my supervisors at SCA R&D Centre, Bo Westerlind and Peter Sandström, my supervisor at Luleå University of Technology in Skellefteå, Olov Karlsson. Another helpful person I would like to thank is professor Per Gradin at Mid Sweden University. Last but not least, I also give a special thank to the people who works at the Pulp and Paper testing group at SCA without whom this study would not have been possible.

Ann Axelsson
Skellefteå
December 2008

Abstract

This degree project concerning evaluation of strength potential in paper made by mechanical pulp based on fibre properties has been carried out at SCA R&D Centre in Sundsvall.

In the mechanical pulping process, the energy consumption and the strength properties of the paper depend on the raw material. To evolve the process towards lower energy consumption and an improved end product, a greater understanding of the connection between the wood fibres and the paper strength is needed.

In this project, the fibre properties, such as dimensions and strength properties have been characterized and the tensile strength of the final paper has been modelled by modifying the Page and the Shear-lag model as well as with multivariate analysis.

The methodology of this study was to collect data from mechanical pulps with a wide range of freeness levels. The fibres were characterized by their dimensions length, width and cell wall thickness, but also properties like curl, kink, fibrillation, slenderness ratio and collapsibility. The strength of fibres as well as the interfibre bonds were measured. Model building followed the measurements and the final models were tested using an independent set of pulps.

It was found that the Page model for predicting tensile strength index could be improved by expanding the expression for fibre strength to incorporate Z-parameter and curl index and by expanding the interfibre bond strength expression to incorporate fibrillation index and curl index.

The best model to use is Shear-lag whether in its original form or by simplifying it to resemble three serial connected resistors consisting of fibre strength, interfibre bond strength and fibre deformation.

Content

1 Introduction

In the production of paper, wood fibres retain most of their original structure. The tree species and individuals determine the range of fibre structure and dimensions modified by the pulping process and therefore the properties of the final paper product. For a fibre network to arise, bonding between fibres is of great importance. These bonds sprung from the tendency of cellulosic fibres to bond to each other during drying from polar liquids like water. Although fibres and bonds are very important, paper cannot be seen as a collection of fibres attached to one another, since the properties of both fibres and bonds are affected by the structure they form. In other words, the mechanical properties of a fibre dried individually differ from a fibre cut from a paper sheet. When the paper dries, local internal stresses develop and act within and between fibres changing the properties of both fibres and bonds. The internal stresses depend on the anisotropic shrinkage potential of the fibres and on the external stresses applied on the paper during drying. However, macroscopically the net stress is zero. When it comes too mechanical pulping, it is an energy consuming process that results in paper with good optical properties, but with not so good strength properties. To decrease the energy consumption during the pulping process and to increase the strength of the final paper product the understanding of the mechanisms behind the formation of fibre networks has to increase.

The aim for this project carried out at SCA R&D Centre in Sundsvall was to develop a model to predict the tensile strength for paper based on fibre geometry and material properties to enable future development of the mechanical pulping processes.

2 Background and theory

The goal of the pulping process is to liberate the fibres from the wood matrix and to make them suitable for papermaking. The dominating pulping processes are mechanical or chemical. In mechanical pulping the yield ranges from 90% to nearly 100%, since only easily dissolved carbohydrates and extractives are lost. Unfortunately it requires a lot of external energy. For chemical pulps the yield is lower because nearly half of the raw material is dissolved in the process, on the other hand, the degradation products is commonly used for energy production. Generally mechanical pulp is produced at the paper mill and tailor-made for the end purpose while chemical pulp is manufactured in a few major grades and is often refined at the paper or board mill to improve fibre bonding and paper strength.

Some of the benefits with mechanical pulp compared to chemical pulp are the high yield leading to low raw material cost, high light scattering, good formation and a large volume. The drawbacks are the need for a high quality raw wood material, high consumption of electrical energy, lower paper strength, limitations in bleaching, brightness instability and that the pulp often contains impurities.

2.1 Mechanical pulping

The main principle behind mechanical pulping is to break down the structure to fibres and fines by subjecting the wood raw material to mechanical forces. There are two major methods of producing mechanical pulp; by pressing wood logs against a revolving pulpstone (grinding), and by disintegrating wood chips in a disc refiner (refining). Figure 1 shows a schematic example of a stone grinder, and Figure 2 shows a schematic example of a double disc refiner. Grinding results in a pulp with good optical properties but with a low strength, while refining results in a pulp with good strength but with poorer optical properties. The major mechanical pulping processes are listed in Table 1.

Table 1. Nomenclature for mechanical pulps. The yield values are for fresh debarked Norway spruce wood and closed processes with a water usage 10-20m^3/metric ton.

GW (SGW)	**Stone Groundwood** Atmospheric grinding of logs using a pulpstone. The temperature of the shower water is normally 70-75˚C. Yield 98.5%.
PGW	**Pressure Groundwood** Logs are ground in pressurized conditions at a shower water temperature lower than 100˚C. Yield 95.5%.
TGW	**Thermo Groundwood** Atmospheric grinding of logs with shower water temperatures of 80˚C or more. Yield 98.5%.
RMP	**Refiner Mechanical Pulp** Atmospheric refining of chips using a disc refiner with no other treatment then washing of chips and perhaps some atmospheric presteaming before refining. Yield 97.5%.
PRMP	**Pressure Refiner Mechanical Pulp** As RMP, but pressurized refining at an elevated temperature. Yield 97.5%.
TMP	**Thermomechanical Pulp** Chips are preheated with (pressurized) steam and refined under pressure at elevated temperatures at 110-155˚C. Yield 97.5%.
CMP	**Chemimechanical Pulp** 1. General name for all chemimechanical pulps, produced by refining or grinding of chemically pretreated wood. Yield 80-95%. 2. Pulp that is manufactured from chemically and normally also thermally pretreated chips by refining under atmospheric or pressurized conditions. Relatively strong chemical treatments are used. Yield typically lower than 90%.
CTMP	**Chemithermomechanical Pulp** Pressurized refining of chemically pretreated chips or coarse pulp. Relatively mild treatments. Yield typically over 90%.

In an ideal mechanical pulping process the wood fibres are separated from each other with a retained fibre length and they also have to be delaminated (internal fibrillation). At the same time a large amount of fines with suitable bonding and light scattering characteristics must be produced from the middle lamella and the primary and secondary wall while the remaining secondary wall has to be fibrillated (external fibrillation).

The characteristics of paper from mechanical pulp are low density, high stiffness, high opacity, good absorption of ink and a good printability. The major use for mechanical pulp is mechanical printing papers such as newsprint and magazine paper. Other uses are board grades, wallpaper, soft tissue, and absorbents. Since it has low strength qualities it is sometimes reinforced with chemical pulp.

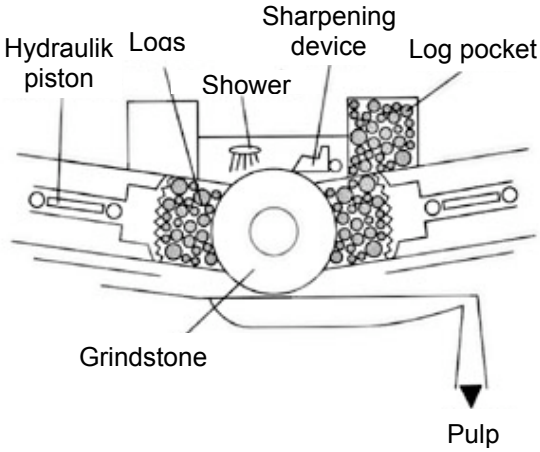

Figure 1. *Stone grinder*

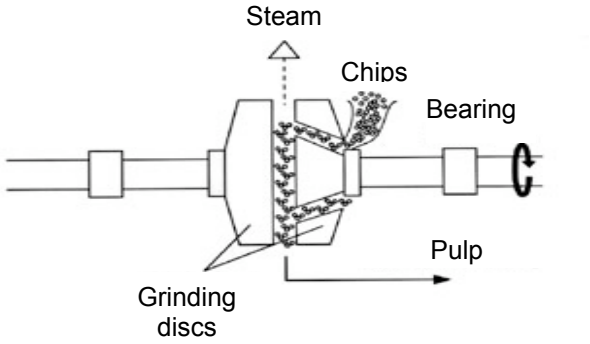

Figure 2. *A chip refiner with one stationary and one rotating disc.*

2.2 Bleaching

There are mainly three reasons for bleaching pulp; one is to make the paper whiter to increase the contrast between ink and paper in printing. Another reason is that pulp contains impurities which otherwise can turn out as dots in the paper. The third reason is to reduce the effects of aging because paper has a tendency to become yellow and brittle over time, primarily due to lignin. Bleaching can be done either by removing lignin or by modification of the lignin structures that absorbs light, where the latter is used on mechanical pulp.

2.3 Paper production

In a paper machine the fibres are consolidated to form a web. Paper can be manufactured using only wood fibres, but additives are sometimes used to enhance certain properties. The diluted pulp is spread out over a moving wire, which is an endless woven cloth. In this stage some water is drained before the fibre web is pressed between rolls on a felt, which removes the water more effectively. To further reduce the water content of the fibre web, the paper is dried on steam-heated cylinders (Figure 3).

To decrease the paper thickness and make the paper smoother most papers is nipped between iron rolls, this is called calendering. For further smoothening of the surface, some paper is covered with a coating colour, filling hollows in the surface.

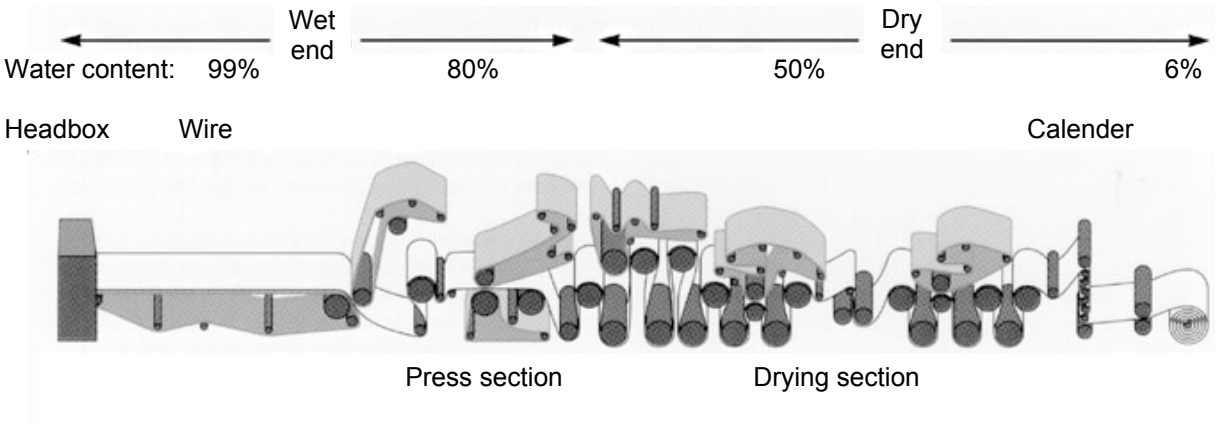

Figure 3. *A simplified picture of a paper machine without a coating section.*

2.4 Pulp properties

Since the mechanical pulping process is fairly harsh, the pulp consists of more or less intact fibres, fibre fragments and fines. The properties of a mechanical pulp depend on the quality and the quantity of these fibre fractions that varies to a great extent between different processes. The fibres give the pulp strength and can be characterized by their length, surface texture, and the softness of the fibre wall. Unfortunately the pulp also consists of undeveloped coarse fibres and shives (bundles of fibres). These defects can cause cracks in the paper and induce dusting during printing, they also affects the surface smoothness and the appearance of the paper.

Wood is a viscoelastic, natural polymeric material so the effect of mechanical impact depends on temperature, moisture and time under load. The transition temperature where the polymers abruptly changes from stiff to soft is very important since the stiffness have a great effect on the fibre characteristics. The transition temperature depends on the moisture content, temperature and frequency of the grinder or refiner. In absolute dry conditions the transition temperature for cellulose range from 200°C to 250°C, for hemicellulose the range is from 150°C to 220°C and for lignin the corresponding values are 130°C to 205°C depending on the degree of crystallinity. Water has a plasticizing effect lowering the transition temperatures as the water content increases (Metso Paper inc, Viljanmaa 2003). Since the fibre walls are fully saturated during the production of mechanical pulp, the hemicelluloses and the cellulose softens at a temperature of 20˚C, which makes the transition temperature of lignin the most important one. Water saturated spruce lignin softens at a temperature of 90˚C measured at a frequency of 0.5 Hz (Sundholm 1999). An increase in frequency leads to an increase in the transition temperature.

2.4.1 Fibre properties

As the fibres are separated from the wood matrix their characteristics are determined depending on where the fracture takes place. At low temperatures where the lignin is stiff, the fractures are uncontrollable leading to a large amount of broken fibres and fines. Since the fibre surface is ruff with a small amount of lignin the bonding capacity is good. This is typical for RMP since the production temperature is around 100˚C with a frequency in the proximity of 100 Hz. For processes like TMP, where the temperature is higher, the fracture zone is in the outer S1 layer or in the primary wall (Figure 4) leading to longer fibres, in the optimal case the original fibre length. The characteristics of the lignin can be changed with chemicals towards a lower glass transition temperature, and for CTMP the fracture zone is in the middle lamella leading to a smaller amount of shives and smooth fibre surfaces with a high amount of lignin that reduces the bonding capacity.

Independent on the process, more mechanical treatment leads to more fines and more flexible fibres since lamellar cracks are developed and the outer layer gets peeled of reducing the circumference.

Slenderness

The slenderness ratio, λ is a way to characterize the slenderness of a fibre. It is defined as the ratio between the surface area, Pl and the cross sectional area of the fibre wall, A_w.

$$\lambda = \frac{Pl}{A_w}, \tag{1}$$

where P is the circumference and l is the fibre length.

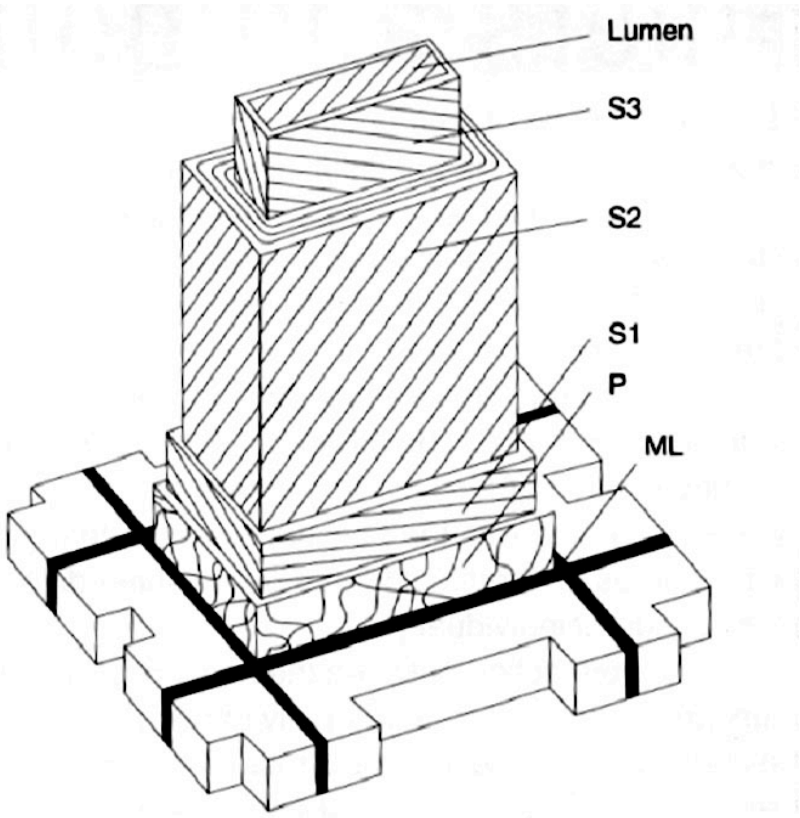

Figure 4. *Cellwall structure of a wood fiber (conifer tracheid). ML, middle lamella; P, primary wall; S1, S2, S3, layers of secondary wall.*

Latency

During the pulping process, the fibres are exposed to stresses and becomes compressed, twisted and curled. These deformations can also arise during the thickening of the pulp. Curls are smooth bends of the fibres while kinks change the direction abruptly and form an angle. Curl is commonly measured with the curl index, *CI* given by the formula

$$CI = \left(\frac{l_c}{l_p} - 1 \right) * 100\%, \tag{2}$$

where l_p is the projected length of a fibre, and l_c is the contour length (Figure 5).

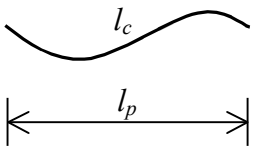

Figure 5. *A curled fibre with projected length, l_p and contour length, l_c.*

Kink index, *KI* is calculated by the formula

$$KI = \frac{n_1 + 2 * n_2 + 3 * n_3 + 4 * n_4}{l_c} \tag{3}$$

where

n_1 is the number of 10-20˚ kinks in a fibre,

n_2 is the number of 21-45˚ kinks in a fibre,

n_3 is the number of 46-90˚ kinks in a fibre, and

n_4 is the number of >90˚ kinks in a fibre.

Fibre strength

The pulping process affects the strength of fibres, the elastic modulus, tensile strength, and breaking strength of individual fibres, since they are affected by inhomogeneities they achieve during the process and natural defects in the cell wall. Deformations, like curl and kinks, reduce the fibres ability to carry and transmit load, since they get a reduced effective fibre modulus and an increased effective rupture elongation.

Collapsibility

There are several ways to express fibres collapsibility. A very straightforward way is the collapse index that is a precise measurement on how much a fibre has collapsed. It is calculated by the formula

$$Collapse\ index = 1 - \frac{LA}{LA_0},$$

where LA is the lumen area after collapse, and LA_0 is the original lumen area. The drawback with the collapse index is the need for measurements before and after collapse where the latter is difficult to attain. Other possible candidates for collapsibility parameters indicate a fibres tendency to collapse and not the actual collapse. Both the Z-parameter and the collapse resistance, CR are based on the cross-sectional geometry.

The Z-parameter is defined as the ratio between the cross-sectional area of the fibre wall, A_w and the total cross-sectional area, A_c.

$$Z = \frac{A_w}{A_c} \tag{4}$$

If the fibre is assumed to have a circular cross section, the collapse resistance is calculated as:

$$CR = \frac{2cwt^2}{2r - cwt}, \tag{5}$$

where cw$t$ is the cell wall thickness and r is the fibre radius. The fibre is assumed to have the same elastic modulus through the entire fibre wall, and an ideally plastic behaviour. The relation between the Z-parameter and the collapse resistance for a fibre with a circular cross-section is

$$CR = fw\frac{\left(1 - \sqrt{1 - Z}\right)^2}{1 + \sqrt{1 - Z}} \tag{6}$$

where fw is the fibre width. Fibre collapse leads to a decrease in optical properties of paper, since the cell lumen of uncollapsed fibres scatter light.

Fibrillation

There are two types of fibrillations, internal and external. When fibres are exposed to mechanical treatment local damages can arise in the fibre wall, internal fibrillation, and the fibre surface can unravel causing fibrils to partly loosen from the cell wall, external

fibrillation (Figure 6). The level of external fibrillation is determined with the fibrillation index, *FI* that is calculated as:

$$FI = \frac{A_{Fibr}}{A_F} * 100\%,$$

where A_{Fibr} is the area of the partially loosened material, and A_F is the total area of the fibre. External fibrillation occurs in water suspension and when the water is removed the external fibrils return to the fibre surface.

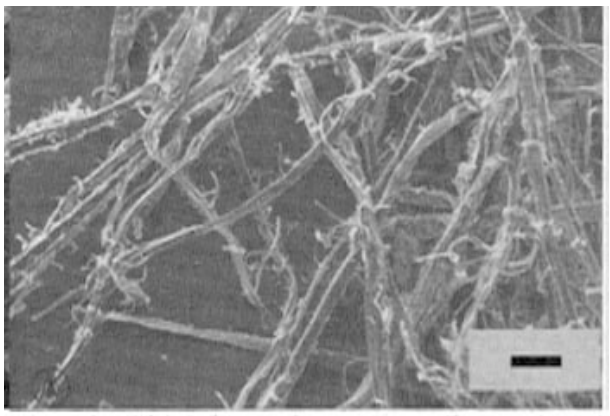

Figure 6. *TMP fibres freeze-dried to reveal external fibrillation. The bar at bottom right is 100 μm long.*

2.4.2 Fines

Fines are defined as the fraction of pulp that passes a 200-mesh Bauer-Mc-Nett wire screen and have therefore a length under 0.20 mm. In mechanical pulp, fines originate from the middle lamella and the primary wall and contribute to 20-40 % of the weight. The amount of fines depends on where in the wood matrix the fibres are separated. If the fracture is in the secondary or primary wall the amount of fines is smaller then if the fracture is in the middle lamella . The fines act as a binder and scatter light.

2.5 Paper formation and strength

The strength properties for paper are expressed as the strength to density ratio also called the specific strength or tensile strength index, σ_T^w. For the in-plane specific tensile strength the calculation is

$$\sigma_T^w = \frac{\text{Ultimate load/unit sample width}}{\text{Grammage}} = \frac{\sigma_T}{\rho_s},$$

The strength depends on the strength of individual fibres as well as the strength of the interfibre bonds.

2.5.1 Interfibre bonds

When fibres are so close to each other, a few Å apart, that hydrogen bonding, van der Waals' interaction and molecular entanglements can occur, an interfibre bond can be created. These bonds do not only hold the paper together, they also affect the optical, electrical and dimensional properties of the paper and depends of pulping, refining, pressing and drying. The final structure of interfibre bonds is a composition of S1-S1, S1-S2 or S2-S2 layers and they consists of entangled and inter-penetrating microfibril bundles, fibrils, fines and colloid

material crossing over between fibres. If the fibres are flexible, a wrap-around-type of bond can be created and in some bonds, the network structure can induce shear strains.

The formation of interfibre bonds starts when the solid content of the pulp increases in the paper making process. At first the surface tension pulls the fibres closer together as the water is removed, the Campbell-effect. Fines and fibrillation working as a link between the fibre surfaces aid the formation of bonds. The bonding formation is influenced by fibre-water interactions and it is possible that fibres have long polymeric chains (60-80 nm) extending from the surface into the water. The Campbell-effect is gradually changed into hydrogen bonds, but exactly at which solid content this happens is still unknown (Vainio 2007).

Since fibres shrink laterally, shear stresses are evolved in the bonding area (Giertz 1964). The level of shrinkage depends on how much water the fibre walls contain, which also depends on the fibrillation and the chemical composition of the fibre wall. The shrinkage forces are largest in the bonding edges and this is the first area to take load at strain. In freely dried sheets, the shrinkage stresses generate axial compressive forces in crossing fibres and can cause deformations called microcompressions in bonded fibre segments (Figure 7). These deformations are regions where the alignment of the microfibrils is locally disturbed. The stresses in the bonding area and microcompressions changes the properties in bonded segments making the properties of bonded fibres different than the properties of free fibres.

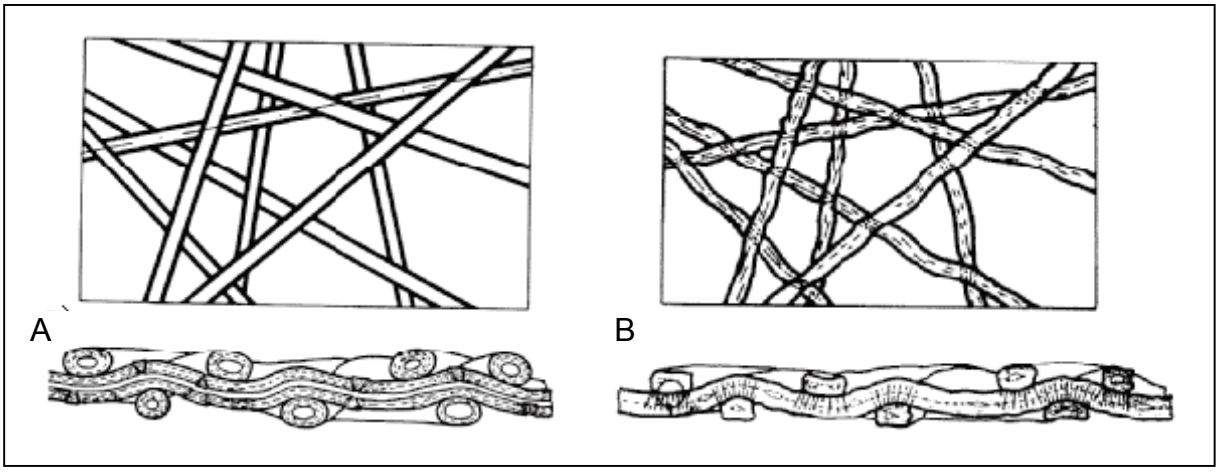

Figure 7. *Schematic plan view and cross-section of paper (A) before and (B) after free drying.*

The interfibre bonding and therefore the strength properties of paper, is improved by internal and external fibrillation. Internal fibrillation leads to a partial delamitation of the fibre wall, which increases the swelling degree, flexibility, and conformability of the wet fibre wall. External fibrillation can unravel the surface structure of a fibre in water suspension and make loose fibril ends to stick out from the fibre wall. Since cellulose surfaces comes closer to each other more hydrogen bonds can occur, which enhances the sheet consolidation.

2.5.2 Activation

Deformed fibres that cannot carry any load can be modified to active components in the network by activation. Activation occurs during drying when the lateral shrinkage of fibres is transmitted to axial shrinkage of neighbouring fibres in the bonding surface. If the shrinkage is restrained, slack fibre segments are straightened since the drying is done under stress (Figure 8). This behaviour is called the Giertz effect (Giertz 1964).

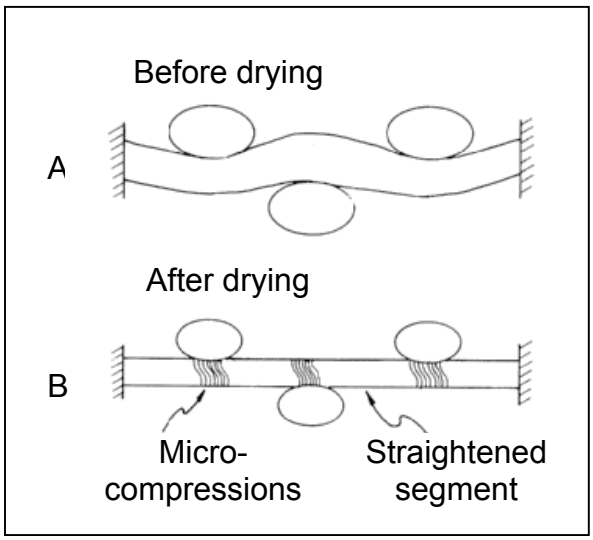

Figure 8. *Schematic fibre (A) before and (B) after restrained drying.*

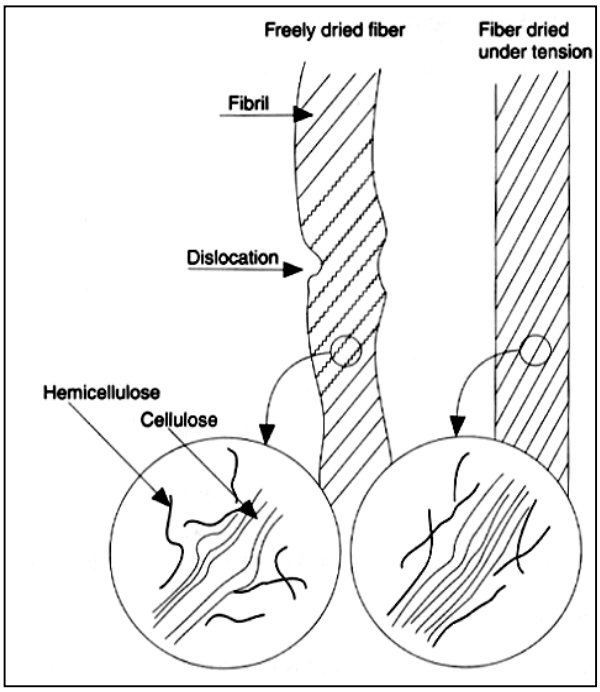

Figure 9. *Schematic representation of the probable structural changes involved in the Jentzen effect.*

Activation leads to a phenomenon called the Jentzen effect (Vainio 2007) where the axial elastic modulus in the fibres increases. This happens because if the fibre is dried under axial load, it is straightened causing dislocations and other defects to be pulled out. Also the fibril angle is reduced and the cellulose and hemicellulose chains rearrange and align themselves parallel with the external load (Figure 9). All this leads to an improvement of the fibres capacity to carry load and makes the load-elongation curve more linear.

Maximizing the bonded area and fibre length can increase, while deformations like kink and curl can decrease the activation process (Vainio 2007). Deformed fibres also lead to a nonuniform load distribution decreasing the networks ability to carry load since they cause local stress points. The aim is a pulp with low coarseness, and wide and straight fibres.

2.5.3 Densification of paper structure

During wet pressing and drying the densification of the paper structure is determined by collapsibility, adaptableness, flexibility, straightness of wet fibres and swelling. The fibres ability to adapt and collapse depends on cross-sectional dimensions, internal fibrillation, and the cell walls morphology and chemical composition. High adaptableness and collapsibility leads to a denser paper. Curled fibres lead a lower density because it creates voids in the structure.

The degree of swelling depends on the chemical composition and internal fibrillation. When fibres swell, the water attaches hydroxyl groups in the cell wall. Lignin contains few OH-groups, only one ore two per 10 carbon atoms, making it difficult for the water to bond to the lignin molecules. Cellulose and hemicellulose contain three OH-groups per six carbon atoms. Weak internal bonds in hemicelluloses makes the OH-groups readily available, while stronger internal bonds in crystalline cellulose makes the availability lower. The saturation moisture content in lignin is characteristically 10%, while it is 30% in cellulose and 80% in hemicelluloses at a temperature of 20˚C and a relative humidity of 100% (Niskanen 1998). In other words, lignin inhibits swelling and hemicelluloses promote it.

2.6 Paper strength models

There are several models trying to explain the correlation between the fibre properties in pulp and the tensile strength properties of the final paper. The Page model and the Shear-lag model are two of them (Page 1969, Calsson, Lindström 2004).

2.6.1 Page

According to Page's theory (Page 1969) the tensile strength of a paper depends on the fraction of broken fibres in the zone of rupture, which depends on both the strength of individual fibres and the strength of the bonds between them. The model is based on two assumptions, where the first deals with the distribution of stress in a paper strip at the moment of tensile failure.

As a paper is exposed to strain, bonds are breaking in the end of fibres causing the load to increase in the remaining fibres. As the load reaches the rupture strain on the fibres oriented parallel to the load, the paper fractures. Mathematically this can be written as:

$$\sigma_T^w = \frac{n_f Z_c}{\left(n_f + n_p \right)} = \left\{ Z_c = \sigma_{ZS}^w \left(1 - \mu^2 \right) \right\} = \frac{n_f \sigma_{ZS}^w \left(1 - \mu^2 \right)}{\left(n_f + n_p \right)},$$

where

σ_T^w is the tensile strength of the strip [Nm/kg],

n_f is the number of fibres crossing the rupture zone that take load at failure and break,

n_p is the number of fibres crossing the rupture zone being pulled out since they do not carry any load due to bond breakage,

Z_c is the finite-span tensile strength of the strip if no bonds had broke [Nm/kg],

σ_{ZS}^w is the zero-span tensile strength [Nm/kg], and

μ is the Poisson's ratio.

The Poisson's ratio is theoretically one third for sheets where the fibres have a random orientation, so the tensile strength formula above can be written as:

$$\sigma_T^w = \frac{8}{9} \frac{n_f \sigma_{ZS}^w}{\left(n_f + n_p \right)}. \qquad (7)$$

Depending on the strength of the fibre and the bonding forces between the fibre and the matrix, the fibre will either be pulled out or break. The second assumption deals with the relationship between the number of fibres that break at failure and the number of fibres that is pulled out intact. This can be expressed as:

$$\frac{n_p}{n_f} = F\left(\varphi, \beta \right)$$

where φ is the mean fibre strength [N], and β is the mean force applied along the fibre axis and across the rupture line required to pull a fibre from the sheet [N].

The variable β depends on the relative bonded area of the sheet, the bond strength per unit area, and the fibre length.

Considering the dimensional aspects this can also be expressed as:

$$\frac{n_p}{n_f} = f\left(\frac{\varphi}{\beta}\right) \tag{8}$$

If the fibre strength, φ exceeds the bond strength, β, the fibres are pulled out intact, and when the bond strength exceeds the fibre strength, the fibres break. When the fibre strength and the bond strength are equal, the fibres have equal chances of pulling or failing. Therefore the function has to satisfy the following conditions:

$$\begin{cases} \varphi >> \beta, & f(\varphi/\beta) \to \infty \\ \varphi << \beta, & f(\varphi/\beta) \to 0 \\ \varphi = \beta, & f(\varphi/\beta) = 1 \end{cases}.$$

The simplest function satisfying these conditions are $f(\varphi/\beta) = \varphi/\beta$. This combined with Eqs. 7 and 8 gives:

$$\frac{1}{\sigma_T^w} = \frac{9}{8}\left[\frac{1}{\sigma_{ZS}^w} + \frac{1}{\sigma_{ZS}^w}\frac{\varphi}{\beta}\right] \tag{9}$$

The fibre strength, φ for a random sheet of Hookean fibres is given by:

$$\varphi = \frac{8}{3} A_c \rho \sigma_{ZS}^w, \tag{10}$$

where A_c is the average cross sectional area [m^2], ρ is the density [kg/m^3], and 8/3 is a scale factor due to the random orientation of the fibres in the zero-span test.

The assumption that all fibre-to-fibre bonds acts together along the fibre length, gives the bond strength, β as:

$$\beta = \tau_b P \frac{l}{4}(RBA) \tag{11}$$

where

- τ_b is the shear bond strength per unit bonding area [Pa],
- P is the circumference of the fibre cross section [m],
- l is the fibre length[m], and $l/4$ is the mean pulled length for a straight fibre, and
- RBA is the relative bonded area of the sheet.

Combining Eqs. 9, 10 and 11 gives the final formula for the tensile strength of paper:

$$\frac{1}{\sigma_T^w} = \frac{9}{8\sigma_{ZS}^w} + \frac{12A\rho}{\tau_b Pl(RBA)}. \tag{12}$$

Equation 12 has the structure:

$$\frac{1}{Z} = \frac{1}{Z_1} + \frac{1}{Z_2}$$

which can be recognised from electric circuit theory as parallel resistors indicating that bond strength and fibre strength acts as such.

2.6.2 Shear-lag

Since studies have shown that fibres can be pulled out intact even if the fibre-to-fibre bonds are strong, shear stress could be a limiting factor in paper strength properties. The Shear-lag model was developed for composites but can also be used in prediction of paper qualities (Carlson, Lindström 2004). A central idea in the model is the transfer of load from the matrix into the fibre. The shear stress is assumed to be constant along the fibre length and a linear axial stress is built up in the fibre (Figure 10). If the fibre is short, the axial stress will not reach the ultimate value, σ_f before the fibre is pulled out. On the other hand, if the fibre is long, the fibre breaks, since the axial stress in the fibre is higher than the ultimate stress of the fibre. The critical length, l_{crit}, for a fibre located symmetrically with respect to the fracture plane, is the boundary between the two cases and is defined as:

$$l_{crit} = \frac{\sigma_f d_f}{2\tau_b},$$

where d_f is the fibre diameter[m], and τ_b is the shear strength between the fibres [Pa].

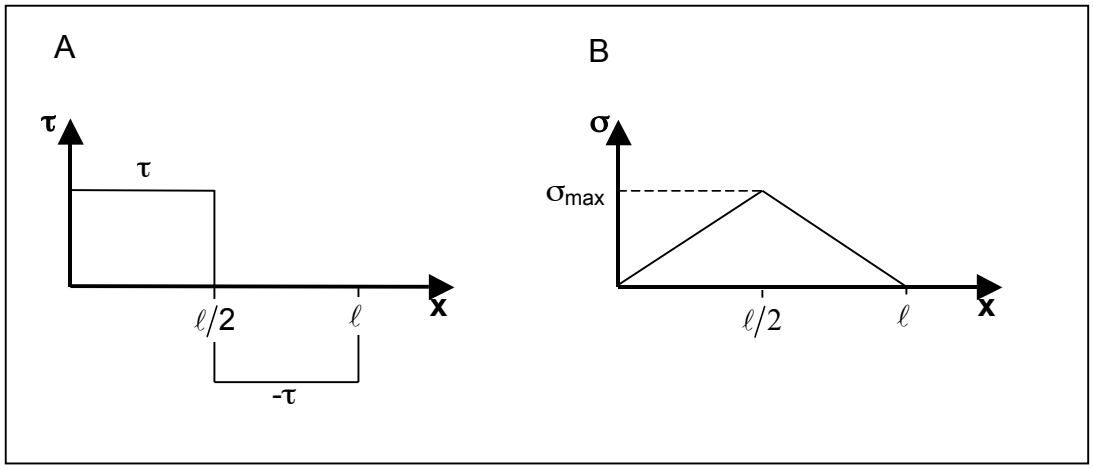

Figure 10. *(A) Fibre/matrix shear stress diagram for short fibres and (B) axial fibre stress diagram for short fibres.*

If the length of the fibres is smaller than the critical length, the tensile strength, X_t is given by

$$X_t = \frac{V_f \tau_b l}{d_f}, \quad l < l_{crit}, \tag{13}$$

where V_f is the volume fraction of fibres. However, at fracture, all fibres bridging the fracture plane will be pulled out from the matrix. If the paper consists of fibres with a length longer than the critical, only fibres with the ends within the distance $l_{crit}/2$ from the fracture plane will be pulled out, the remaining fibres will break. The tensile strength of the composite is:

$$\sigma_{TC} = V_f \sigma_f \left(1 - \frac{l_{crit}}{2l}\right), \quad l > l_{crit}, \tag{14}$$

where the first part is an expression for the breaking fibres, and the second part is an expression for the fibres being pulled out.

Since the fibres in a paper are randomly distributed, the Shear-lag model has to be adjusted. A sheet of paper has the cross-sectional dimensions width, b and thickness, t, and consists of a number, n_f of unidirectional long fibres that break at the same time along the fracture line. The

volume fraction of fibres in a sheet is calculated from the apparent sheet density, ρ_s and the density of the fibres, ρ_c

$$V_f = \frac{\rho_s}{\rho_c}.$$

The tensile strength of the paper, σ_T can, with the disregard of the interactions between the fibres, be calculated by the formula

$$\sigma_T = \frac{n_f F_f}{bt} = \frac{\rho_s}{\rho_c}\sigma_f, \tag{15}$$

where F_f is the tensile load at failure of the fibre.

For papers consisting of short fibres, $l < l_{crit}$, the shear force transmitted to a fibre is given by the relation

$$V = \tau P \frac{1}{2}(RBA), \tag{16}$$

where

τ is the uniform shear stress [N],

P is the cross-sectional circumference [m], and

RBA is the relative bonded area.

When the shear stress equals the fibre-to-fibre bond shear strength, τ_b and the shear force equals the tensile load at failure of the fibre F_f, the critical length is achieved from Eq. 16

$$l_{crit} = \frac{2F_f}{\tau_b P(RBA)}.$$

If the length of the fibres are shorter than the critical, between zero and a half of a fibre will be pulled out and the average value is one forth of a fibre. This makes the average load on a fibre being pulled out become (Eq. 16)

$$V = \frac{\tau_b P(RBA)}{4}.$$

By replacing σ_f with V/A_c in Eq. 15 the failure stress is obtained

$$\sigma_T = \frac{\rho_s Pl(RBA)}{4\rho_c A_c},$$

where A_c is the fibres cross-sectional area.

As the fibres are randomly distributed in the plane, Eqs. 13 and 14 has to be reduced. A factor often used is 3/8. Since the paper structure contains a lot of voids, the strength is often expressed as tensile index or specific strength, defined as the ultimate stress divided by apparent sheet density

$$\sigma_T^w = \frac{\sigma_T}{\rho_s}.$$

Finally the formulas for tensile strength in paper becomes

$$\begin{cases} \sigma_T^w = \dfrac{3\tau_b Pl(RBA)}{32\rho_c A_c}, & l < l_{crit}, \\ \sigma_T^w = \dfrac{3\sigma_f}{8\rho_c}\left(1 - \dfrac{l_{crit}}{2l}\right), & l > l_{crit}, \end{cases} \tag{17}$$

where the critical length is

$$l_{crit} = \frac{2\sigma_f A_c}{\tau_b P(RBA)}. \tag{18}$$

2.6.3 Previous model adaption

In an attempt to make the Page's and the Shear-lag model more usable, they have been adapted to include parameters easier to measure than the original ones. The parameters *RBA* and τ_b is difficult to measure so the product $\tau_b RBA$ which appears in both models is replaced with the Z-strength, σ_{ZD} and water retention value, *WRV* (Westerlind et al 2007). Although the direction of bonding strength is perpendicular to the direction in question it is an indicator of the bonding degree.

To further simplify the models, a circular cross-section is assumed so the slenderness ratio, λ (Eq. 1) becomes

$$\lambda = \frac{Pl}{A_w} = \frac{fw \cdot l}{cwt(fw - cwt)},$$

where *cwt* is the cell wall thickness and *fw* is the fibre width, and mean values are used.

After adaption the Page model is described as

$$\frac{1}{\sigma_T^w} = a_1 \frac{1}{\sigma_{ZS}^w} + a_2 \frac{cwt(fw - cwt)\rho_c}{fw \cdot l \cdot \sigma_{ZD} WRV} \tag{19}$$

where the constants a_1 and a_2 is determined through multiple regression to the values 0.993 and 1.385 respectively.

After modification, the Shear-lag model achieves the appearance

$$\begin{cases} \sigma_T^w = b_1 \dfrac{fw \cdot l \cdot \sigma_{ZD} WRV}{cwt(fw - cwt)\rho_c}, & l < l_{crit}, \\ \sigma_T^w = b_2 \cdot \sigma_{ZS}^w \left(1 - \dfrac{l_{crit}}{2l}\right), & l > l_{crit}, \end{cases} \tag{20}$$

where

$$l_{crit} = b_3 \frac{cwt(fw - cwt)\sigma_{ZS}^w \cdot \rho_c}{fw \cdot \sigma_{ZD} WRV}, \tag{21}$$

and b_1, b_2, and b_3 are constants determined to be 0.523, 0.298, and 0.93.

Nether the original theories nor the modifications consider fibres with defects like curl or kink or consolidation mechanisms.

2.7 Data analyses

Curve fitting is the easiest way to analyse data. The basic idea is to fit N points (x_i, y_i) to a function $\hat{y}\left(x,\{a_j\}\right)$, where $\{a_j\}$ is a set of M parameters which are adjusted to the data at hand. The fit is good if a graph of the data set (x_i, y_i) and the function $\hat{y}$ shows that the curve passes in the proximity of the points. The most common way to obtain a curve fit is with the least square fit, which is finding the function that minimises the residual sum of squares, *RSS*:

$$RSS = \sum_i \left(\hat{y}_i - y_i\right)^2 .$$

Since *RSS* increases with the number of points, it is sometimes normalized to make comparison independent on the size of the data:

$$RSS = \frac{1}{N-1}\sum_i \left(\hat{y}_i - y_i\right)^2 , \qquad (22)$$

where N is the number of data points.

2.7.1 Linear regression

In linear regression, the data set is fit to a straight line:

$$\hat{y} = a_1 + a_2 x + \cdots + a_n x_n$$

The fit parameters can be calculated with matrix algebra:

$$\mathbf{y} = \mathbf{aX} \Leftrightarrow \mathbf{a} = \mathbf{yX}^{-1},$$

where **y** is a row vector containing the n measured y's, **a** is a row vector containing m fit parameters and **X** is a $m \times n$ matrix containing m variables at n measured points.

2.7.2 Multivariate data analysis

A data set consists of N rows and K columns, where the rows are observations and the columns are variables. In multivariate data analyses, data and models can be represented as points, lines, planes, and hyper planes in a multidimensional space where the variables define the axis. This multidimensional space is called the K-space, if the work considers predictors (X-variables) and M-space if the work considers responses (Y-variables). Data in these multidimensional spaces can be projected into a two-dimensional window overviewing the data and therefore making it easier to interpret. To analyze relations between predictors and responses two spaces are needed one for the **X**-block, and one for the **Y**-block, as well as a connection between the two spaces.

The multivariate data analysis tool used in this study to connect the information in the X-variables with the information in the Y-variables is projections to latent structures by means of partial least squares, PLS. The analyses are made in Simca-P 11.5 where the default setting for pre-processing of data is mean-centering and scaling to unit variance. This means that the variables are given equal importance since variables with a higher degree of variance would have a larger influence than variables with smaller diversity otherwise. If variable importance is known on beforehand, scaling should be adjusted accordingly (Eriksson et al 2006).

PLS finds a linear relation between the dependent variables in the **Y**-matrix and the predictor variables in the **X**-matrix, this can be expressed as

$$\mathbf{Y} = f\left(\mathbf{X}\right) + \mathbf{E},$$

where E is a residual matrix.

The objectives of the analysis is to approximate the X and Y spaces well and to maximize the correlation between X and Y. In mathematical terms, this is expressed as

$$\mathbf{X} = \mathbf{1} * \overline{\mathbf{X}} + \mathbf{T}\mathbf{P}' + \mathbf{E}$$

$$\mathbf{Y} = \mathbf{1} * \overline{\mathbf{Y}} + \mathbf{U}\mathbf{C}' + \mathbf{F}$$

$$\mathbf{U} = \mathbf{T} + \mathbf{H}$$

where **T** is a matrix of scores that summarizes the X-variables, **P** is a matrix of loadings that shows the influence of the variables, **U** is a matrix of scores summarizing the Y-variables, **C** is a matrix of weights that summarize the correlation between **Y** and **T**(**X**), and **E**, **F** and **H** are matrices of residuals. In the PLS algorithm, the matrix **W** containing additional loadings, called weights expresses the correlation between **U** and **X** and is used to calculate **T**.

In other words, PLS creates the necessary new components, $\mathbf{t_a}$, that are orthogonal to each other and are made from a linear combination of the X-variables. The t's are used to predict Y. For each component (i), the parameters $\mathbf{t_i}$, $\mathbf{u_i}$, $\mathbf{w^*_i}$, $\mathbf{p_i}$, and $\mathbf{c_i}$ are determined by a PLS algorithm. The scores **t** and **u** carry information about the observations and their similarities or lack of similarities regarding the problem and model at hand. The weights **w*** and **c** contains information about how the variables combine to form the quantitative relation between X and Y. Numerically large w-values indicates important X-variables.

In model evaluation the most important factor is the fraction of the total variation of the Y's that can be predicted by the model, which is the Q^2 value defined as

$$Q^2 = 1.0 - \frac{PRESS}{RSS},$$

where $PRESS$ is the prediction error sum of square calculated by the formula:

$$PRESS = \sum_i \sum_m \left(Y_{im} - \hat{Y}_{im} \right)^2,$$

and RSS is the residual sum of squares given by:

$$RSS = \sum_i \sum_m \left(F_{im} \right)^2.$$

Depending on how good the model is, the Q^2 value approaches 1.0.

To determine the importance of the variables in the X block, VIP-values are commonly used. VIP stands for variable importance in the projection and can be calculated by using:

$$VIP_k = \sqrt{\frac{k \sum_a w_{ak} SS_a}{\sum_a SS_a}},$$

where k is the number of variables, w_{ak} is the weight of the k^{th} variable for principal component a, and SS_a is the sum of squares explained by a. Terms with a large VIP value are more important to the model than terms with a low VIP value.

3. Materials and methods

3.1 Pulps

The models where built using 41 commercial pulps from SCA Ortviken of which 16 were TMP-pulps and 25 were HT-pulps.

For evaluation of the models a total of 12 pulps was used, two CTMP-pulps from SCA Östrand, four pulps from SCA Ortviken and six TMP-pulps from the Metso pilot plant in Sundsvall were used. These pulps span a wide range of freeness levels and are made from pine (Pinus silvestris) and spruce (Picea abies). All pulps are tabled in Appendix A.

3.1.1 Measurement of fibre properties

The dimensions and properties like kink and curl was measured using Fiberlab™, which is an image analyses system. In Fiberlab™ a highly diluted sample flows through a capillary where length measurement optics detects the presence of a fibre and follows its way through the capillary. When the fibre reaches the optic sections centre, a Xenon lamp flashes. Two CCD-cameras captures an image of the fibre simultaneously, one for length measurements and one for cross-sectional measurements. The results are calculated via image analyses in the equipments software.

3.1.2 Water retention value, WRV

Water retention values where measured using the SCAN-C 62:00 with the exception that tap water was used instead of ionized water. In the test, pulps are dewatered under suction to a dry content of 5-15 %, and then centrifuged for 15 minutes. The mass of the sample is measured before and after drying. It is calculated by

$$WRV = \frac{m_1}{m_2} - 1,$$

where m_1 is the mass of the centrifuged sample before drying, while m_2 is the mass of the dry sample. WRV is a measurement of how much water the fibre walls can absorb and therefore their draining ability on the wire.

3.1.3 Canadian standard freeness, CSF

Canadian Standard Freeness, which is described in standard ISO 5267-2 was also used to determine drainage. A suspension containing 3.00 ± 0.002 g pulp is diluted to 1000 ml and filtrated through a funnel with two openings, one at the side, and one in the bottom. The freeness is the volume of the filtrate flowing through the side opening and measured in ml.

3.2 Paper making and testing

3.2.1 Test sheets

The test sheets with grammage 65 g/m^2 where made with recirculated white water and formed in a standard sheet former on a wire screen under suction. Then they where exposed to a pressure of 1.89 MPa in 5 + 2 minutes before it was dried in a temperature of 23°C and a relative humidity of 50%, all according to the ISO-5269 standard method.

3.2.2 Mechanical testing

All mechanical testing were made in a controlled climate at a temperature of 23°C and a relative humidity of 50%.

Grammage

Grammage was measured by weighing a test sheet with a known area with a scale with high accuracy.

$$\text{Grammage} = \frac{m}{A},$$

where m is the mass of the sheet and A is the sheets area. This method is explained in standard ISO 5270:99. Grammage is used to index the properties tensile strength and zero-span tensile strength.

Z-strength, σ_{ZD}

The out of the plane tensile strength, the Z-strength was measured according to the SCAN-P 80:98 standard. Double-coated adhesive tape was used to attach metal clamps to both sides of the specimens. The clamps were then pulled apart and the force needed to delaminate the test sheet was recorded. The Z-strength is a measurement of bond strength in the Z-direction.

Zero-span tensile strength index, σ_{ZS}^{w}

The standard ISO 15361 was used to determine the dry zero-span tensile strength. A pull test where the distance between the clamps initially was zero loaded the specimens until break. The zero-span tensile strength is an indicator of fibre strength.

Tensile strength index, σ_{T}^{w}

To measure tensile strength, the SCAN-P 67:93 standard was used. Test strips were subjected to constant elongation speeds until break.

3.3 Models

3.3.1 Pre-processing of raw data

Commonly, mean values are calculated from measurements divided into classes. These mean values are also used when calculating derived properties. The arithmetic average, $\bar{x}(n)$, the length-weighted average, $\bar{x}(l)$ and the weight-weighted average, $\bar{x}(w)$ is calculated by the formulas:

$$\bar{x}(n) = \frac{\sum_i n_i x_i}{\sum_i n_i}$$

$$\bar{x}(l) = \frac{\sum_i n_i x_1^2}{\sum_i n_i x_i}$$

$$\bar{x}(w) = \frac{\sum_i n_i x_1^3}{\sum_i n_i x_i^2}$$

where n_i is the number of fibres in class i, and x_i is the average value of class i. In this study, the data is not divided into classes, instead the derived properties are calculated fibre by fibre and all mean values calculated thereafter, in other words n_i equals one.

Since the technique of measuring fibre parameters is not flawless, the raw data from FiberLab™ was subjected to cleaning. Initially all fibres without measured cell wall thickness was excluded before mean values of fibre length, fibre width, cell wall thickness, slenderness ratio, Z-parameter and collapse resistance were calculated. Mean values for curl index and kink index was calculated for those remaining fibres where the apparatus had been able to perform the measurements. It was assumed that the deformation distribution was constant throughout the samples.

3.3.2 Multivariate analyse of data

In the training set there are several corresponding variables, deformations can be measured using the curl index or the kink index, collapsibility is given by Z-parameter and collapse resistance while water retention value and freeness indicates draining ability.

According to multivariate analyses kink index, *KI* was a better variable than curl index, *CI* since it had a higher *VIP*-value (Figure 11). However there are still some difficulties in measuring *KI*, in FiberLab™. *CI* is measured for approximately 10 times as many fibres than *KI*, so for now *CI* is more accurate to use.

By using collapse resistance, *CR* instead of Z-parameter the models became slightly better. Since *Z* is dimensionless while *CR* is not and the difference was minor, the Z-parameter was used in the model.

When it comes to the choice between water retention value, *WRV* and freeness, *CSF*, models containing freeness had improved predictability compared to models containing water retention value. In this study, only mechanical pulp is considered and in that area freeness is commonly measured and CSF often characterizes pulps degree of refining. These two factors speak on the behalf of freeness. For an equation to be balanced, the right hand and the left hand side has to have the same dimension. However CSF on the right hand side has the

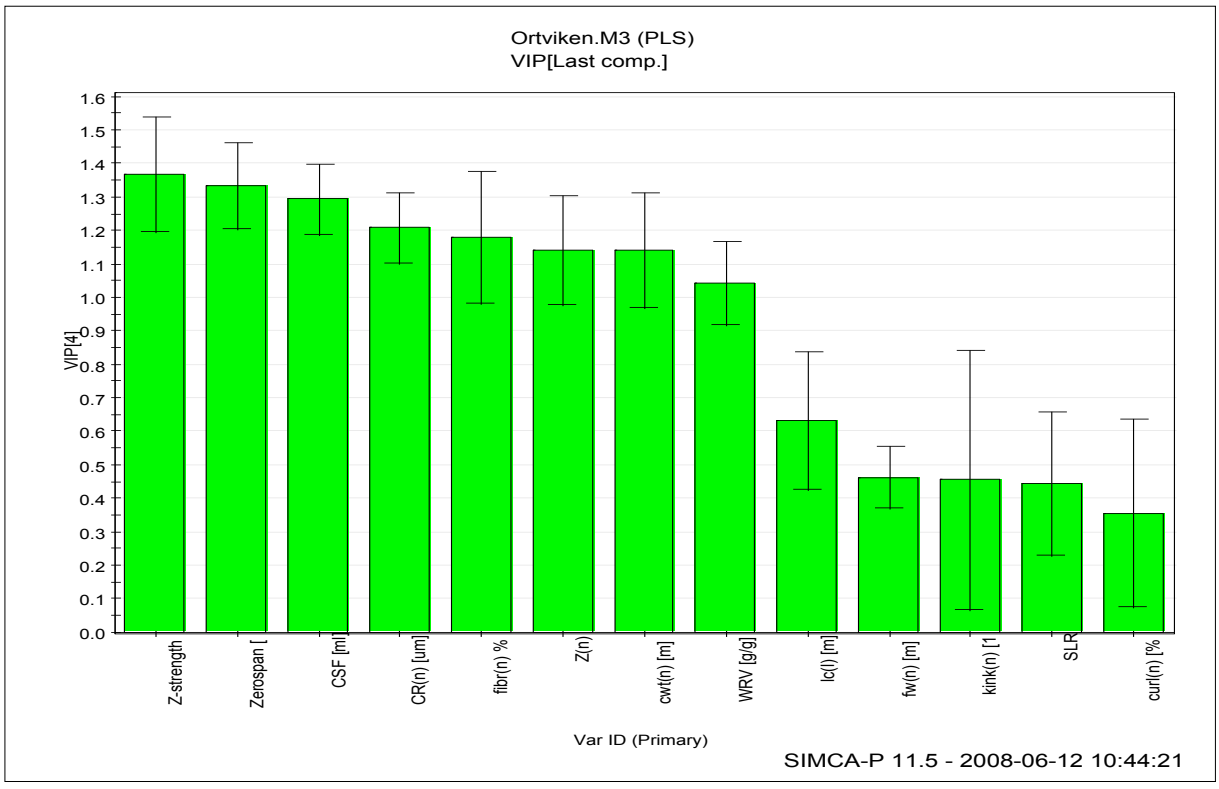

Figure 11. *VIP plot for the variables the models were based on. For clarity, only the most important weight for every variable is shown.*

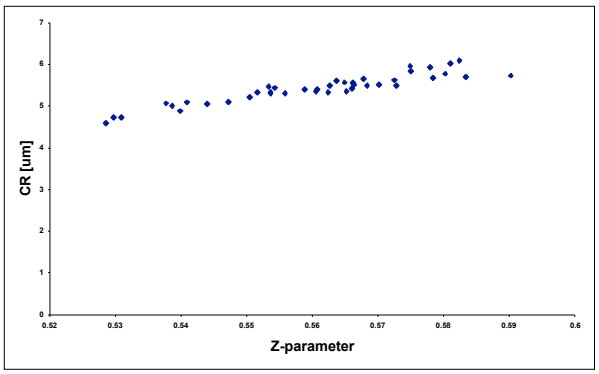

Figure 12. *Collapse resistance versus Z-parameter*

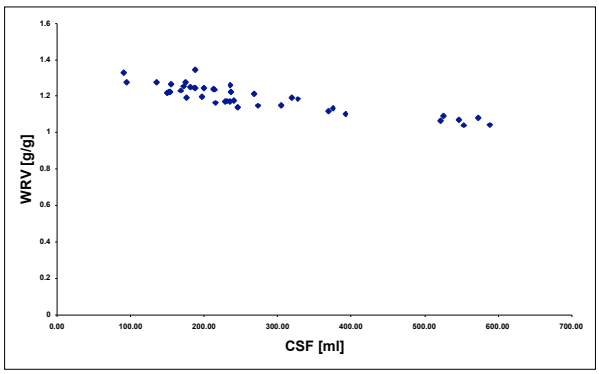

Figure 13. *Water retention value versus freeness*

dimension ml while the tensile strength index on the left hand side has the dimension Nm/kg. The easiest way to handle this deviation in dimensions is to make the CSF term dimensionless, which was done with the 3.00 ± 0.002g dry mass used in the freeness test and the density of the wood fibres in the same test, commonly approximated with the density of cellulose.

$$CSF * 10^{-6} \frac{\rho_c}{3 * 10^{-3}} = \frac{CSF * \rho_c}{3 * 10^3}$$

There are however, correlations between Z-parameter and collapse resistance (Eq. 6 and Figure 12) as well as between water retention value and freeness (Figure 13).

The final multivariate model, MS (Figure 14) became:

$$\sigma_T^w = a_1 CI + a_2 FI + a_3 Z + a_4 \frac{\sigma_{ZD}}{\rho_c} + a_5 \sigma_{ZS}^T + a_6 \frac{CSF * \rho_c}{3000}, \qquad (23)$$

where a_1, a_2, a_3, a_4, a_5 and a_6 are constants determined by multiple regression (Table 1).

Table 1. *Multivariate statistics model constants*

Constant	Value
a_1	-2.38
a_2	4.07
a_3	-20.6
a_4	98.7
a_5	0.595
a_6	0.0177

Table 2. *Variable importance for the multivariate statistics model*

Variable	Importance
σ_{ZS}^T	1.16
$\frac{\sigma_{ZD}}{\rho_c}$	1.15
$\frac{CSF * \rho_c}{3000}$	1.11
FI	1.02
Z	0.965
CI	0.351

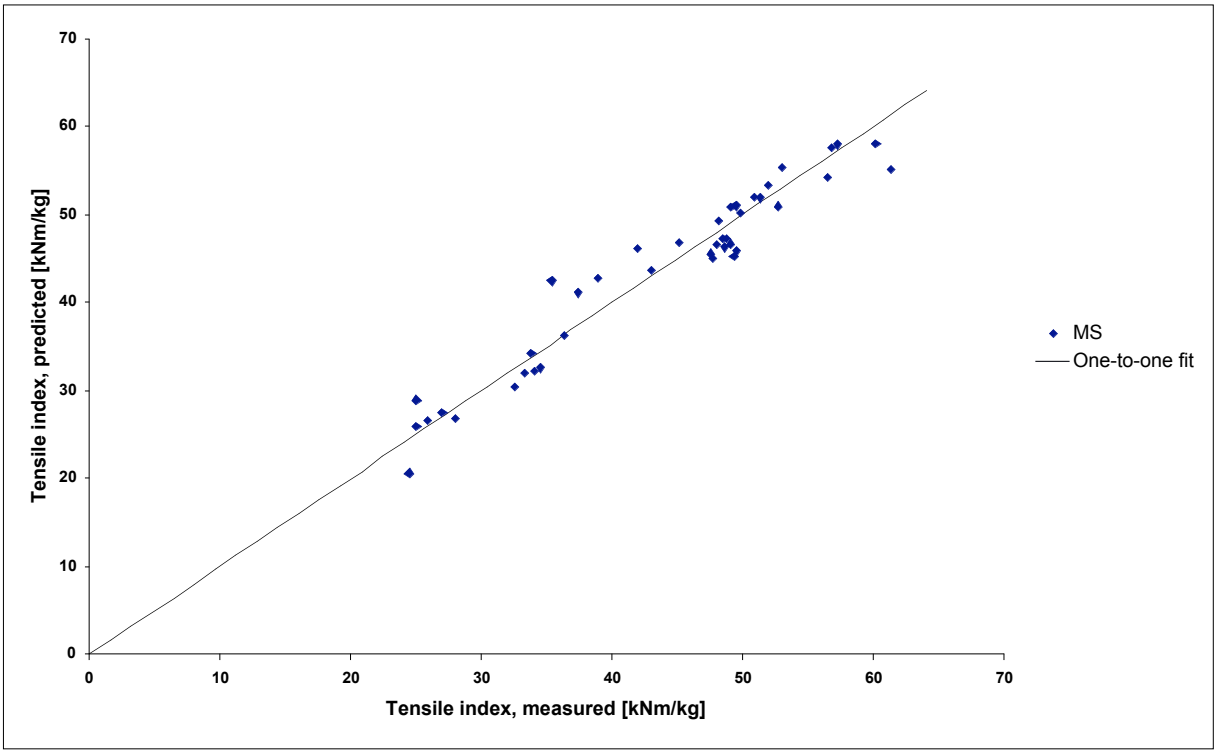

Figure 14. *Predicted tensile index versus measured tensile index for the Multivariate Statistics model, MS*

3.3.3 Modification of existing models

The tensile strength is a combination between fibre strength and interfibre bond strength. In both the Page and the Shear-lag model these two components can be considered as separate terms.

$$\sigma_T^w = f\left(\sigma_{fs}^w, \sigma_{bs}^w\right)$$

where σ_{fs}^w is the fibre strength tensile index and σ_{bs}^w is the interfibre bond strength tensile index. In this study, the models where modified in three ways, the first was simply replacing the product $\tau_B RBA$ with σ_{ZD}, the second was to expand the fibre strength and the interfibre bond strength expressions and the third way was to add a fibre deformation factor. In the previous work by Westerlind et al water retention value was used to improve the models, however *WRV* and *CSF* are measurements on how much the fibres have been processed in the mill. The level of processing used in these models was given by fibrillation, Z-parameter and curl index. External fibrillation is increased and Z-parameter is decreased by refining, while curl index is increased by refining and decreased by latency treatment. All constants were determined by multiple linear regressions and are given in Table 3.

To be able to compare the models with fibrillation, curl and collapsibility to models without, the Page and Shear-lag models where adapted to the available data by substituting $\tau_B RBA$ with the easier measured σ_{ZD} in equations 12, 17 and 18. The first adapted Page model, P1 (Figure 15) became:

$$\frac{1}{\sigma_T^w} = b_1 \frac{1}{\sigma_{ZS}^w} + b_2 \frac{cwt(fw - cwt)\rho_c}{fw \cdot l \cdot \sigma_{ZD}} \qquad (24)$$

where b_1 and b_2 is constants (Table 3). The first adapted Shear-lag model, SL1 (Figure 16) became :

$$\begin{cases} \sigma_T^w = c_1 \dfrac{fw \cdot l \cdot \sigma_{ZD}}{cwt(fw - cwt)\rho_c}, & l < l_{crit}, \\ \sigma_T^w = c_2 \cdot \sigma_{ZS}^w \left(1 - \dfrac{l_{crit}}{2l}\right), & l > l_{crit}, \end{cases} \tag{25}$$

where

$$l_{crit} = c_3 \frac{cwt(fw - cwt)\sigma_{ZS}^w \cdot \rho_c}{fw \cdot \sigma_{ZD}}, \tag{26}$$

and c_1, c_2 and c_3 are constants (Table 3).

The P1 and the SL1 models were used to expand the fibre strength and the bond strength expression to the second adapted Page model, P2 and the second adapted Shear-lag model, SL2.

In the zero-span tensile strength test, the transversal size of the fibres affects the result, so to better approximate the strength in individual fibres, the Z-parameter was used. Fibre strength depends on latency which is given by curl index. The fibre strength tensile index expression was expanded to:

$$\sigma_{fs}^w = k_{fs} \frac{\sigma_{ZS}^w}{Z * CI},$$

where k_{fs} is a constant.

Further the strength of the interfibre bonds depend on latency and fibrillation, so the expanded interfibre bond strength expression became:

$$\sigma_{bs}^w = k_{bs} \frac{\lambda * \sigma_{ZD} * FI}{\rho_c * CI},$$

where k_{bs} is a constant.

The P2 model (Figure 15) became :

$$\frac{1}{\sigma_T^w} = \frac{1}{\sigma_{fs}^w} + \frac{1}{\sigma_{bs}^w} = d_1 \frac{Z * CI}{\sigma_{ZS}^w} + d_2 \frac{\rho_c * CI}{\lambda * \sigma_{ZD} * FI}, \tag{27}$$

where d_1 and d_2 are constants (Table 3).

With the use of an electric circuit analogy, Page can be considered as parallel-connected resistors, while Shear-lag can be considered as serial connected resistors, where the "resistors" in this case is fibre strength and interfibre bond strength. This analogy was used to simplify the original Shear-lag model before expansion to the SL2 model (Figure 16):

$$\sigma_T^w = \sigma_{fs}^w + \sigma_{bs}^w = e_1 \frac{\sigma_{ZS}^w}{Z * CI} + e_2 \frac{\lambda * \sigma_{ZD} * FI}{\rho_c * CI} \tag{28}$$

where e_1 and e_2 are constants (Table 3).

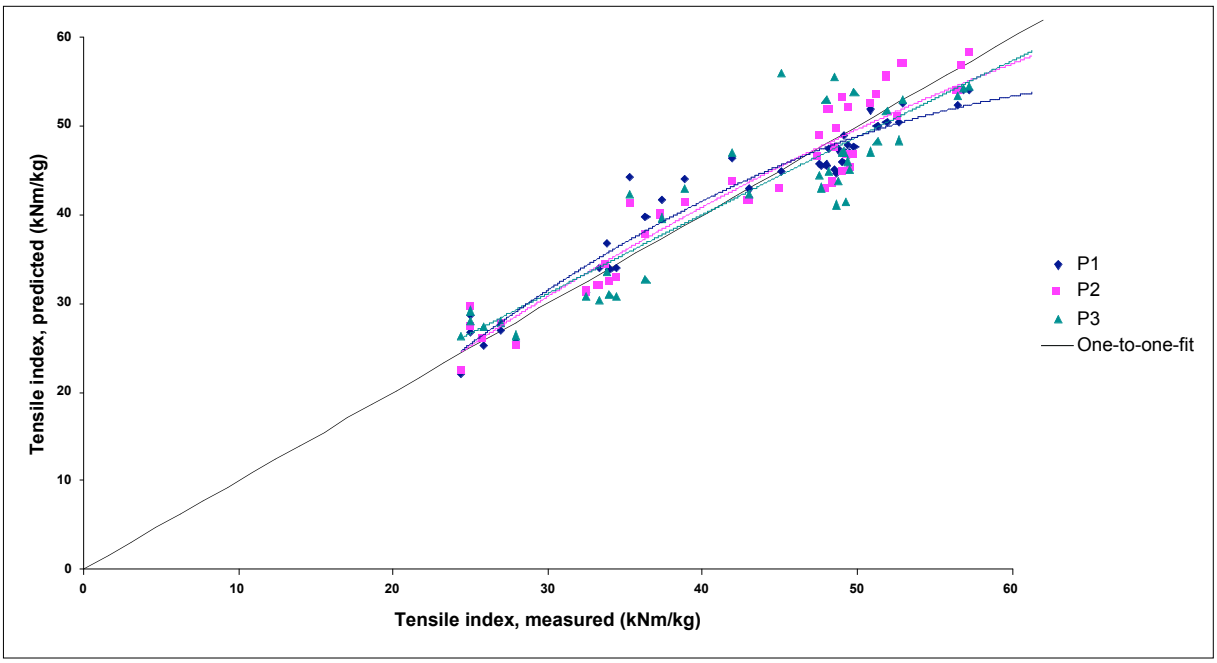

Figure 15. *Predicted tensile index versus measured tensile index for the Page models.*

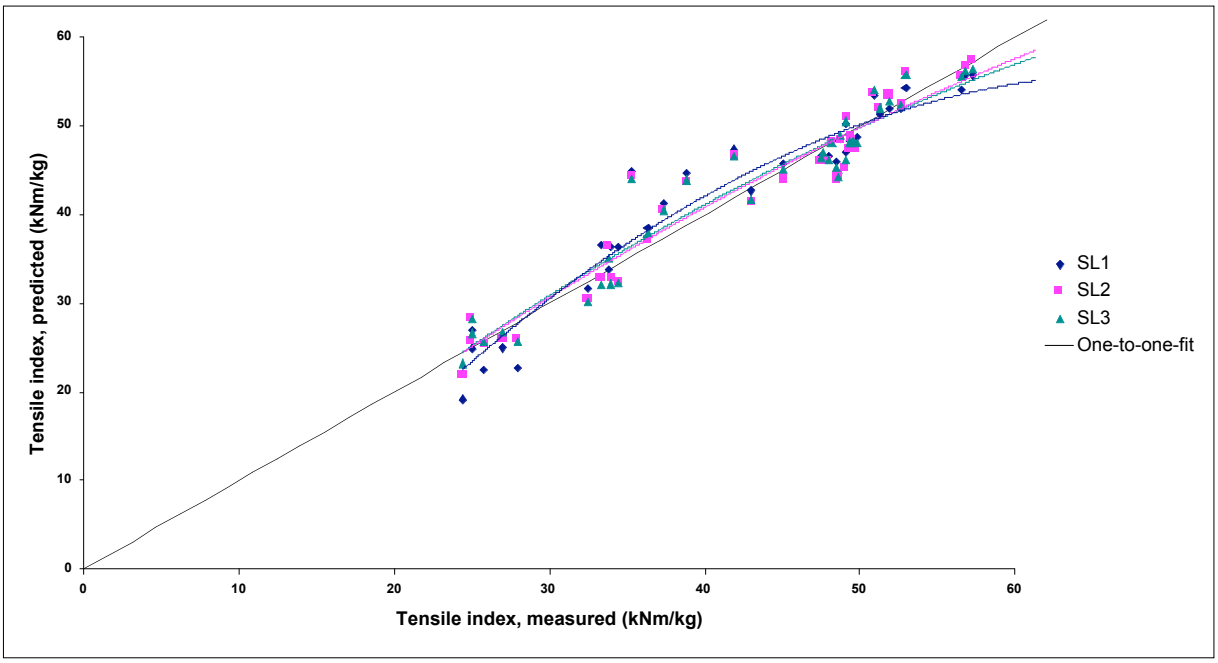

Figure 16. *Predicted tensile index versus measured tensile index for the Shear-lag models.*

For the third adaption, the P1 and the SL1 models where used again as a base for incorporating fibrillation, collapsibility and deformations like curl and kink by adding a fibre deformation factor, *FD*.

$$\sigma_T^w = f\left(\sigma_{fs}^w, \sigma_{bs}^w, FD\right)$$

As stated earlier, fibrillation is positively correlated, while curl and collapsibility is negatively correlated to tensile strength in paper. This gave the fibre deformation factor the appearance:

$$FD = k_{fd}\frac{FI}{Z * CI},$$

where k_{fd} is a constant.

By adding the new factor to the Page model, the P3 model (Figure 15) gained the appearance:

$$\frac{1}{\sigma_T^w} = \frac{1}{\sigma_{fs}^w} + \frac{1}{\sigma_{bs}} + \frac{1}{FD} = f_1 \frac{1}{\sigma_{ZS}^w} + f_2 \frac{\rho_c}{\lambda * \sigma_{ZD}} + f_3 \frac{Z * CI}{FI}, \quad (29)$$

and the simplified Shear-lag model, SL3 (Figure 16) became:

$$\sigma_T^w = \sigma_{fs}^w + \sigma_{bs}^w + FD = g_1 * \sigma_{ZS}^w + g_2 \frac{\lambda * \sigma_{ZD}}{\rho_c} + g_3 \frac{FI}{Z * CI} \quad (30)$$

where f_1, f_2, f_3, g_1, g_2 and g_3 are constants (Table 3).

Table 3. Coefficients determined by linear regression

Model	**Constants**		
	1	**2**	**3**
P1 (Eq. 24)	1.28	0.948	-
P2 (Eq 27)	0.167	0.190	-
P3 (Eq.29)	0.359	$-1.3*10^{-5}$	0.0207
SL1 (Eqs. 25 - 26)	0.597	0.721	0.75
SL2 (Eq. 28)	0.00792	0.554	-
SL3 (Eq. 30)	0.0965	0.268	12.3

3.3.4 Validation

The models were validated using an external, independent test set.

4 Results

In these study two effective models based on Shear-lag theory was found, SL1 and SL3.

As can be seen in Table 4, the models that achieved the smallest normalized residual sum of squares, *RSS* for the training set of pulps was based on Shear-lag theory followed by Page based models. The worse training set model was built by multivariate statistics.

With some exceptions the test pulps drew the same picture. The very simplified Shear-lag model with a fibre deformation factor was very good with both sets of pulps.

Table 4: Normalized residual sum of squares, RSS for the models.

Model	**RSS**	
	Training set	**Test set**
MS	68.3	190
P1	10.5	699
P2	10.0	89.2
P3	16.8	172
SL1	9.96	16.5
SL2	7.72	220
SL3	7.57	16.8

5 Discussion

The multivariate statistics model worked best for pulps from SCA Ortviken (Figure 17), which comes as no surprise since they are very similar to the ones the model is based on. They are manufactured in the same factory, the same refiners and with similar raw material. The most deviating pulps where made at a different factory, SCA Östrand with a different pulping process, CTMP. Another difference between the Ortviken and Östrand pulps is the high freeness values of the CTMP-pulps, 450 and 700 ml (Table A2), while the rest of the set had a freeness ranging from 52 to 218 ml. The deviations could be an effect of either the difference in processes or freeness. For the pulps originating from the Metso Pilot Plant with a similar pulping process the model was stable but far too pessimistic.

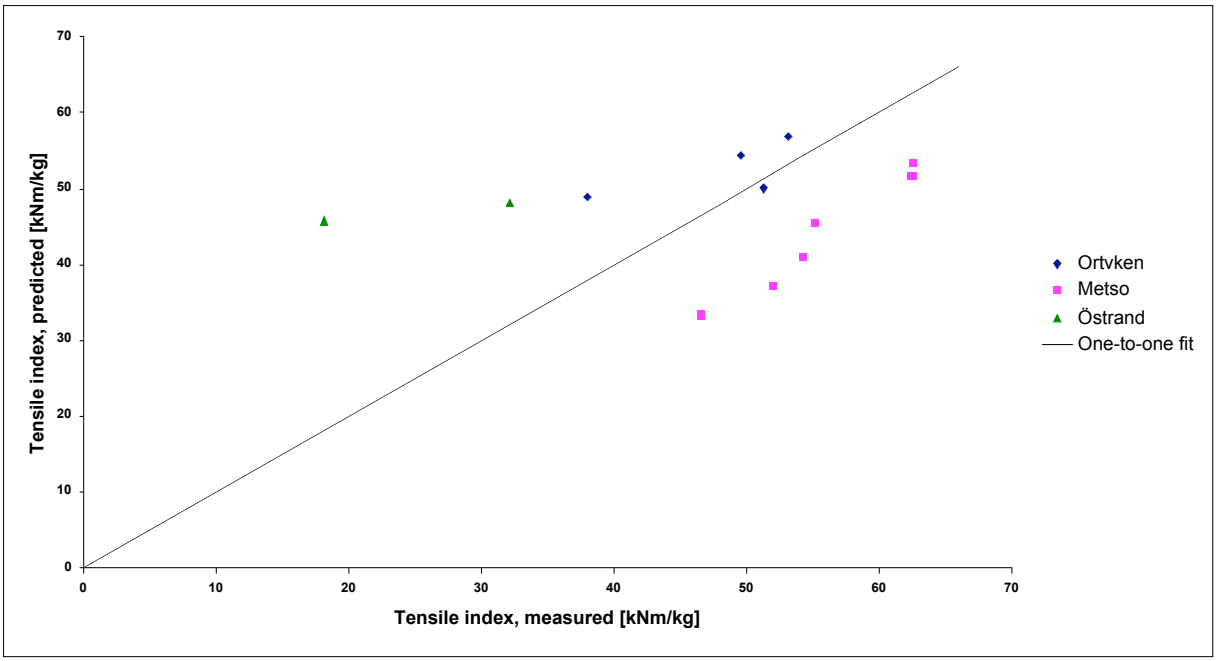

Figure 17. *Predicted tensile index versus measured tensile index for the Multivariate statistics model, for pulps of different origin in the test set.*

The Page based models had large differences between the *RSS*-values of the training pulps and the test pulps, indicating that the Page model is not the best way to explain the connection between fibre properties and tensile strength in paper (Figure 18 and Table 4). The electric circuit analogy suggested by Page in 1969 with fibre strength and bond strength working as parallel resistors is not a correct correlation. For the original form of the Page model, P1 the model was both unstable and optimistic. The best result based on Page theory proved to be the variety with extended variables, P2 which worked similarly well for CTMP and TMP pulps (Figure 19). The difficulties with the P3 model sprung from the low interfibre bond strength coefficient, f_2 underrating the contributions from the bonds on tensile strength.

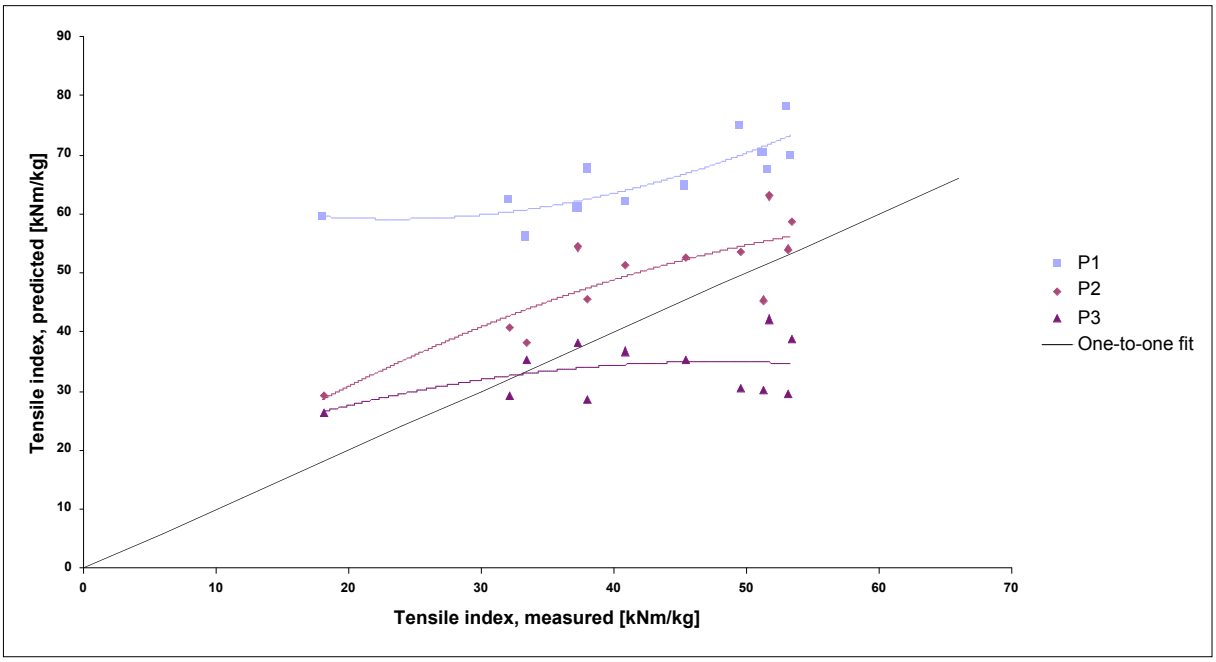

Figure 18. *Predicted tensile index versus measured tensile index for the Page based models used on the test set.*

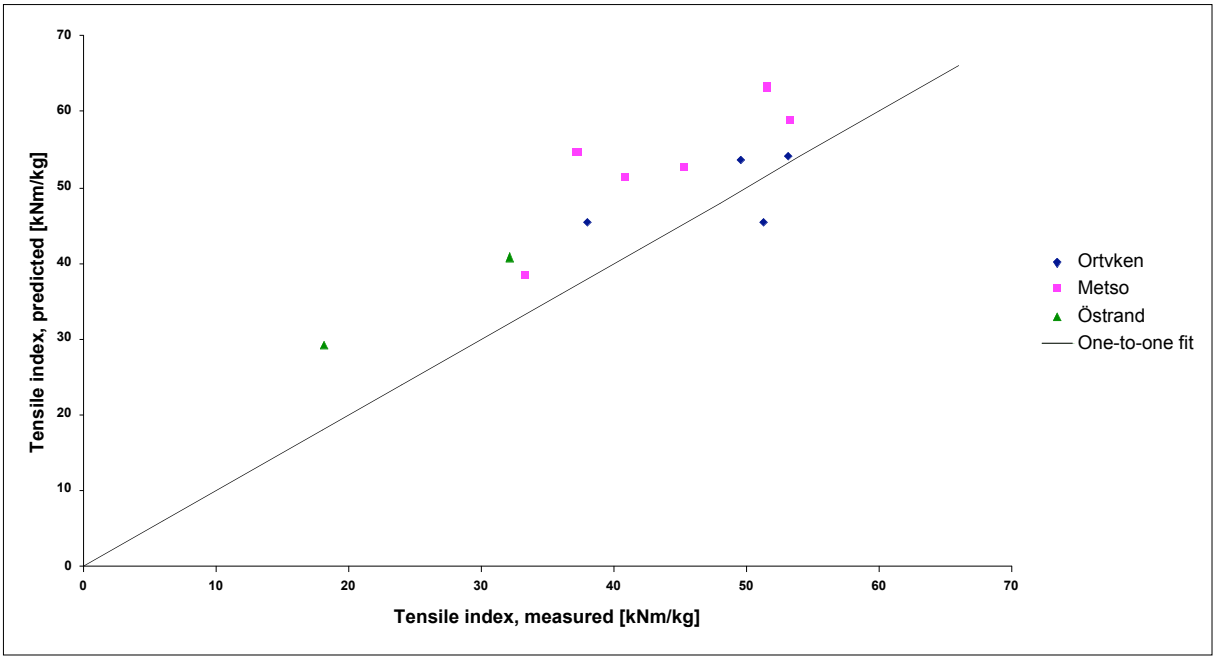

Figure 19. *Predicted tensile index versus measured tensile index for the P2 model, for pulps of different origin in the test set.*

As stated in the results section, the best models sprung from Shear-lag theory, (Figure 20), where both the original model, SL1 and the very simplified version, SL3 with a fibre deformation factor stood out for the test pulps. For neither version the production processes seem to matter (Figure 21 and 22), they work just as good for TMP and CTMP pulps. One should keep in mind that the use of the SL3 model is restricted to pulps with curled fibres since the fibre deformation term approaches infinity as curl index approaches zero. The idea with extending the fibre strength and the interfibre bond strength expression, SL2 was however not successful. That could be an effect of the similarity between the pulps on which the model is built, since the fibre length span is very narrow no critical length could be found.

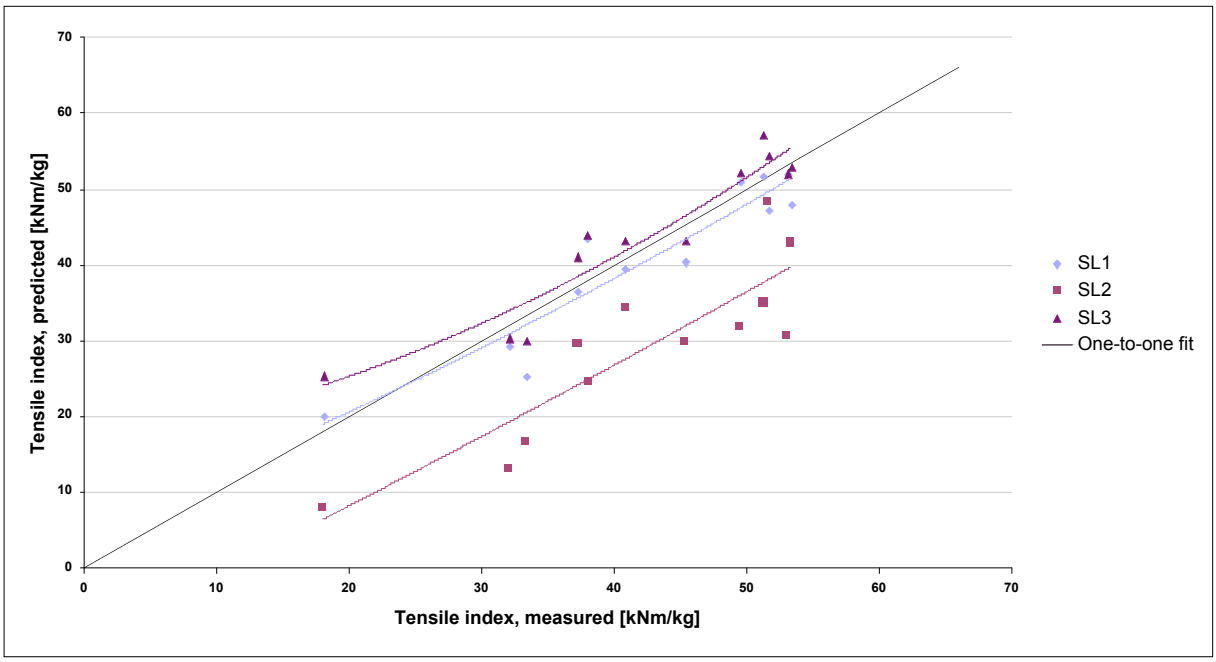

Figure 20. *Predicted tensile index versus measured tensile index for the models based on Shear-lag theory.*

6 Conclusion

For the set of pulps used in this study, it was not possible to build a good model using multivariate statistics, since it only worked reasonably for pulps from the same factory.

The Page model was improved by adding collapse index, Z-parameter and fibrillation index. The best way was to expand the fibre strength and the interfibre bond strength expressions, P2.

For Shear-lag there is no easy answer if it needs to be expanded. The best model of all was the one where $\tau_B RBA$ simply was replaced with σ_{ZD}. A model that was as good, but at the same time easier since it only uses one equation independent of critical fibre length was the simplified Shear-lag model with fibre deformation factor, SL3. Since Shear-lag model SL1 gave a good prediction without using fibre curl or fibrillation the effect of fibre network activation is small for the tested papers made of mechanical pulps.

6.1 Future work

In this study only mechanical pulp with a narrow span of fibre dimensions has been used. The question is how well these models work for chemical pulps and a less homogeneous set of fibres with more extreme fibre dimensions.

Since all extended Page and Shear-lag models include the curl index in the denominator they only work for pulps where the fibres have curls or kinks, which makes the use a bit restricted. If they are to be developed further to include straight fibres as well, this has to be dealt with.

Another drawback with these models is that test sheets have to be made to measure zero-span and Z-directional strength. If the sheets has been made it is easy to measure tensile index instead which makes the model redundant. The next step to develop the models further for these kinds of pulps would be to find alternative ways to determine fibre strength and bond strength.

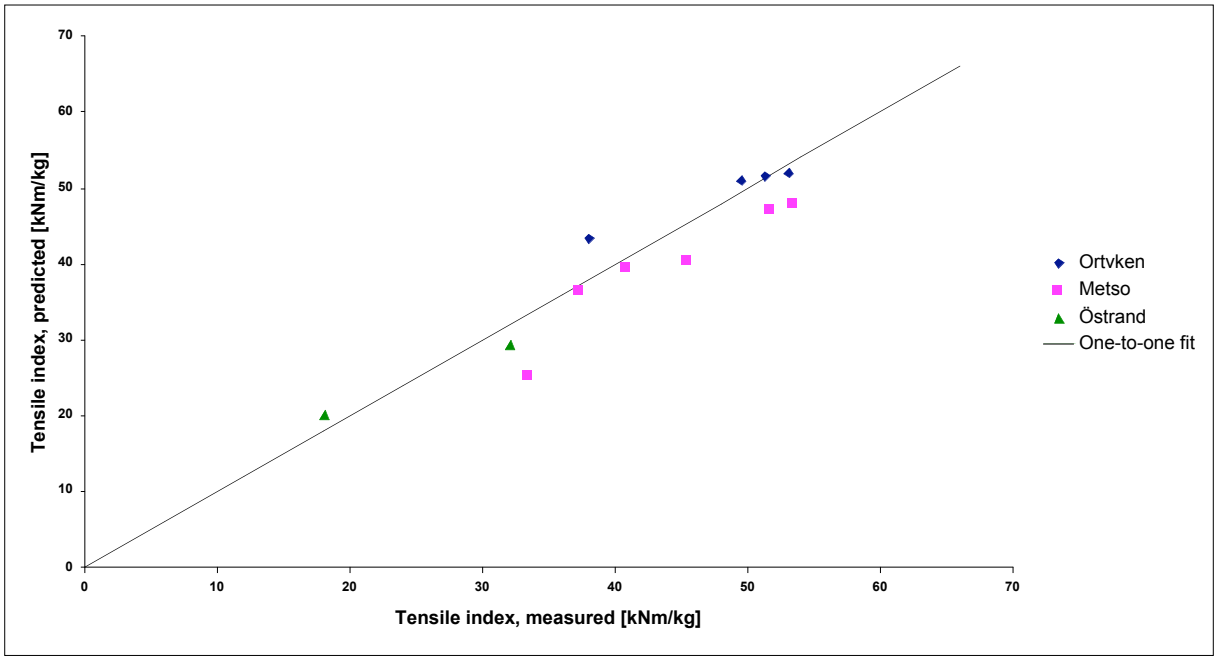

Figure 21. *Predicted tensile index versus measured tensile index for the SL1 model where the pulps are diverted according to their different origins.*

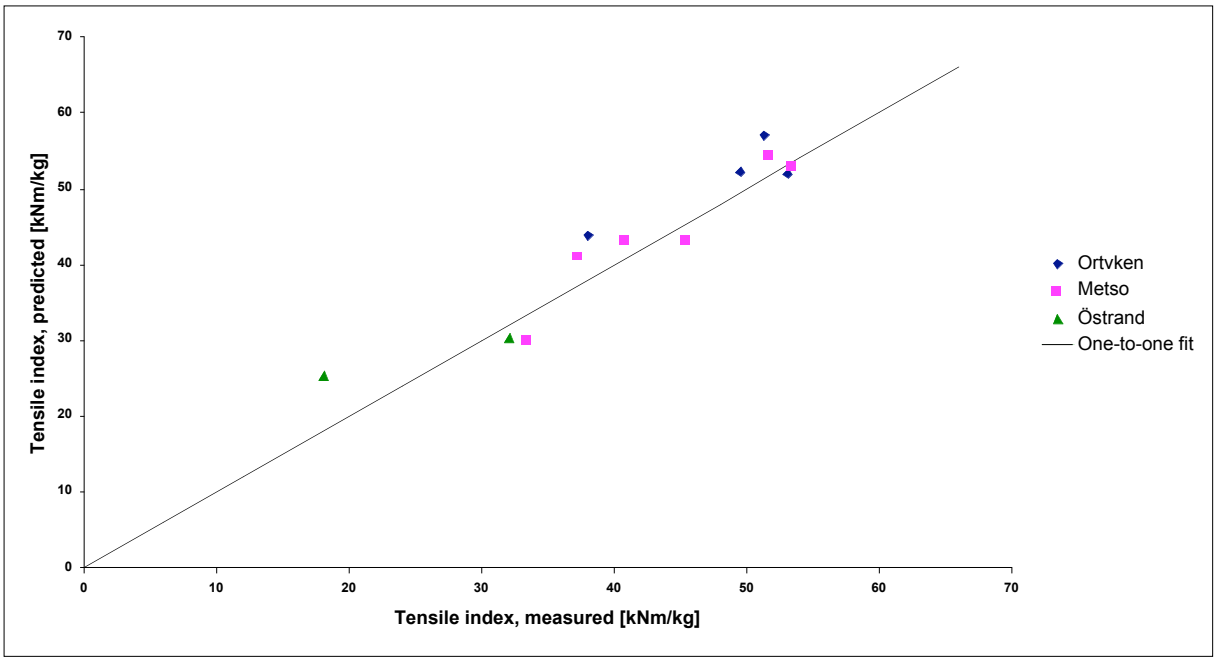

Figure 22. *Predicted tensile index versus measured tensile index for the SL3 model where the pulps are diverted according to their different origins.*

7 References

Carlsson L. A., Lindström T, *A shear-lag approach to the tensile strength of paper*, Composites science and technology 65:183-189, 2005

El-Hosseiny F, *Influence of the "Giertz effect" on development of short-span compression strength*, Tappi 81(2): 177-180, 1998

Eriksson B et al, *Multi- and megavariate data analysis. P. 1, Basic principles and applications*, Umetrics Academy, Umeå, 2006

Gavelin G, Sundstedt K, *Mekaniska massor: framställning och användning*, Skogsindustrins utbildning i Markaryd AB, Markaryd, 1996

Gietz, H.G., *Ännu ett sätt att se på malningsprocessen*, Norsk Skogsindustri 18(7):239-248, 1964

Gärd J, *The influence of Fibre Curl on the Shrinkage and Strength Properties of Paper*, Master thesis Luleå, Luleå University of Technology, 2002

Joutsimo O et al, *Effects of fiber deformations on pulp sheet properties and fiber strength*

Kobets L.P., Deev I.S., *Carbon fibres: structure and mechanical properties*, Composites Science and Technology 57(12): 1571-1580, 1998

Metso Paper inc, Viljanmaa M, *A method for calendering paper on board*. FI 20035029, 2003

Mohlin U-B et al, *Fiber deformation and sheet strength*, Tappi 79(6):105-111, 1996

Niskanen, K (ed.), *Paper physics*, Fapet, Helsinki, 1998

Page D.H, *A theory for the tensile strength of paper*, Tappi 52(4):674-681, 1969

Sundholm J (ed.), *Mechanical pulping*, Fapet, Helsinki, 1999

Trita-FPT-report, Department of Fibre and Polymer Technology, Royal Institute of Technology [Institutionen för Fiber- och polymerteknologi, Tekniska högskolan i Stockholm], Stockholm, 2004-2007

Vainio A, *Interfibre bonding and fibre segment activation in paper – Observations on the phenomena and their influence on paper strength properties.* Doctoral thesis. Helsinki, Helsinki University of Technology , 2007

Westerlind B et al, *Engineering approach to Page and shear-lag theory for predicting tensile strength of paper*. In: International Paper Physics Conference. 2007. Gold Coast, Australia.

Appendix A. Pulps

Table A1. Pulps used in the training set, l is the fibre length, CI is the curl index, FI is the fibrillation index, λ is the slenderness ratio, Z is the Z-parameterand CSF is the Canadian standard freeness.. All values are the arithmetic averages, except for the fibre

Name	Type	Factory	l (l) (mm)	*CI* (%)	*FI* (%)	*λ*	*Z*	*Z-strength* (kN/m^2)	*Zero-span* (kNm/kg)	*CSF (ml)*	*Tensile index (kNm/kg)*
07-M33-A	TMP	SCA Ortviken	1.86	15.9	5.35	464	0.566	344	96	181	38.8
07-M33-B	TMP	SCA Ortviken	1.95	15.5	5.29	467	0.571	299	96	212	37.3
07-M33-C	TMP	SCA Ortviken	1.86	15.9	5.41	462	0.565	374	99	187	41.9
07-M33-D	TMP	SCA Ortviken	2.08	15.3	4.83	499	0.569	254	96	375	36.3
07-M33-E	TMP	SCA Ortviken	2.31	14.2	4.73	562	0.561	126	92	573	25.0
07-M33-F	TMP	SCA Ortviken	2.07	16.3	5.47	485	0.576	227	94	327	33.7
07-M33-G	TMP	SCA Ortviken	2.30	14.1	4.67	529	0.580	124	87	546	24.9
07-M-33-I	TMP	SCA Ortviken	2.12	15.3	4.98	491	0.578	194	93	369	34.4
07-M-33-J	TMP	SCA Ortviken	2.27	14.0	4.59	552	0.576	107	90	552	25.7
07-M-33-K	TMP	SCA Ortviken	2.02	15.8	4.93	479	0.569	200	93	305	33.3
07-M-33-L	TMP	SCA Ortviken	2.26	13.9	4.59	524	0.583	125	90	525	26.9
07-M-33-N	TMP	SCA Ortviken	2.12	14.9	4.96	506	0.565	164	90	392	32.4
07-M-33-O	TMP	SCA Ortviken	2.24	13.9	4.56	506	0.593	99	81	588	24.4
07-M-33-P	TMP	SCA Ortviken	2.03	15.6	4.99	490	0.564	194	92	318	33.9
07-M-33-Q	TMP	SCA Ortviken	2.26	14.6	4.54	519	0.578	115	92	521	27.9
07-M-33-R	TMP	SCA Ortviken	1.90	16.2	5.46	473	0.567	339	96	187	35.3
07-M42-A	HT	SCA Ortviken	2.18	14.1	5.38	558	0.548	308	105	214	49.4
07-M42-B	HT	SCA Ortviken	2.13	14.0	5.41	564	0.539	351	104	186	51.8
07-M42-C	HT	SCA Ortviken	2.21	14.3	5.29	558	0.553	274	101	245	48.5
07-M42-D	HT	SCA Ortviken	2.04	15.2	5.30	453	0.581	321	98	240	43.0

Name	Type	Factory	l (l) (mm)	*CI* (%)	*FI* (%)	λ	*Z*	*Z-strength* (kN/m^2)	*Zero-span* (kNm/kg)	*CSF (ml)*	*Tensile index (kNm/kg)*
07-M42-E	HT	SCA Ortviken	1.73	15.4	5.23	407	0.574	408	96	134	45.0
07-M42-F	HT	SCA Ortviken	1.86	15.0	5.21	411	0.583	406	97	172	48.4
07-M42-G	HT	SCA Ortviken	1.95	15.0	5.30	446	0.576	402	101	175	49.7
07-M42-H	HT	SCA Ortviken	2.11	14.8	5.35	517	0.560	329	98	235	47.4
07-M42-I	HT	SCA Ortviken	1.94	15.8	5.54	432	0.580	397	97	174	47.9
07-M42-K	HT	SCA Ortviken	2.11	15.6	5.54	510	0.563	355	98	199	49.5
07-M42-L	HT	SCA Ortviken	2.20	14.1	5.37	564	0.550	347	103	196	51.2
07-M42-M	HT	SCA Ortviken	2.27	14.3	5.32	564	0.554	321	99	231	48.7
07-M42-N	HT	SCA Ortviken	2.24	14.0	5.22	561	0.555	307	97	273	47.6
07-M42-O	HT	SCA Ortviken	1.92	15.2	5.16	459	0.565	373	98	168	49.0
07-M42-P	HT	SCA Ortviken	2.15	15.0	5.24	543	0.558	333	98	234	49.2
07-M-51-A	HT	SCA Ortviken	2.10	14.9	5.32	555	0.550	378	105	228	50.8
07-M-51-B	HT	SCA Ortviken	1.80	14.7	5.29	520	0.527	419	109	94	60.1
07-M-51-C	HT	SCA Ortviken	1.79	16.0	5.66	504	0.529	421	106	90	61.3
07-M-51-D	HT	SCA Ortviken	2.13	15.0	5.43	536	0.553	373	103	215	52.6
07-M-51-E	HT	SCA Ortviken	1.99	14.9	5.38	537	0.540	403	105	154	56.4
07-M-51-F	HT	SCA Ortviken	2.01	14.5	5.33	543	0.541	401	110	149	56.8
07-M-52-A	HT	SCA Ortviken	2.08	14.2	5.33	564	0.535	381	106	152	52.9
07-M-52-B	HT	SCA Ortviken	2.20	14.0	5.30	568	0.544	304	103	268	48.1
07-M-52-C	HT	SCA Ortviken	2.09	14.3	5.38	560	0.534	388	110	155	57.2
07-M-52-D	HT	SCA Ortviken	2.25	14.1	5.42	574	0.548	325	103	236	49.0

Table A2. Pulps used in the test set, l is the fibre length, CI is the curl index, FI is the fibrillation index, λ is the slenderness ratio, Z is the Z-parameterand CSF is the Canadian standard freeness.. All values are the arithmetic averages, except for the fibre length which is the length weighted mean values

Name	**Type**	**Factory**	**l (l) (mm)**	***CI* (%)**	***FI* (%)**	**λ**	***Z***	***Z-strength* (kN/m^2)**	***Zero-span* (kNm/kg)**	***CSF* (ml)**	***Tensile index* (kNm/kg)**
07-M-52-E	HT	SCA Ortviken	1.57	14.2	5.48	595	0.541	330	102	218	49.4
07-M-52-F	HT	SCA Ortviken	1.54	14.3	5.36	567	0.549	342	106	213	53.0
08-55-D	TMP	SCA Ortviken	1.29	18.2	6.66	502	0.515	455	95	62	51.2
08-55-G	TMP	SCA Ortviken	1.26	14.1	5.32	434	0.561	358	93	165	37.9
W-121	TMP	Metso pilot plant	1.30	10.1	5.71	405	0.597	306	84	149	37.2
W-133	TMP	Metso pilot plant	1.33	11.3	6.85	452	0.575	421	91	51	51.6
W-421	TMP	Metso pilot plant	1.27	11.4	5.80	375	0.593	375	89	139	45.3
W-437	TMP	Metso pilot plant	1.36	12.4	6.78	421	0.576	444	95	54	53.3
W-521	TMP	Metso pilot plant	1.42	10.5	6.25	309	0.684	215	82	198	33.3
W-533	TMP	Metso pilot plant	1.48	10.9	6.43	379	0.650	368	85	63	40.8
T-7050	CTMP	SCA Östrand	1.38	9.6	3.44	398	0.586	133	91	700	18.0
T-7230	CTMP	SCA Östrand	1.28	9.1	3.71	371	0.590	207	90	450	32.0
07-M-52-E	HT	SCA Ortviken	1.57	14.2	5.48	595	0.541	330	102	218	49.4
07-M-52-F	HT	SCA Ortviken	1.54	14.3	5.36	567	0.549	342	106	213	53.0
08-55-D	TMP	SCA Ortviken	1.29	18.2	6.66	502	0.515	455	95	62	51.2
08-55-G	TMP	SCA Ortviken	1.26	14.1	5.32	434	0.561	358	93	165	37.9
W-121	TMP	Metso pilot plant	1.30	10.1	5.71	405	0.597	306	84	149	37.2
W-133	TMP	Metso pilot plant	1.33	11.3	6.85	452	0.575	421	91	51	51.6
W-421	TMP	Metso pilot plant	1.27	11.4	5.80	375	0.593	375	89	139	45.3
W-437	TMP	Metso pilot plant	1.36	12.4	6.78	421	0.576	444	95	54	53.3

Appendix B. Abbreviations and symbols

A_c	Cross-sectional area of a fibre
A_F	Total fibre area
A_{Fibr}	Area of partially loosened material
A_w	Cross-sectional area of the fibre wall
CI	Curl index
CR	Collapse resistance
CSF	Canadian standard freeness
CTMP	Chemithermomechanical pulp
cwt	Cell wall thickness
d_f	Fibre diameter
F_f	Tensile load at failure of a fibre
FI	Fibrillation index
fw	Fibre width
HT	High temperature
KI	Kink index
LA	Lumen area after collapse
LA_0	Lumen area before collapse
l_c	Contour length of a fibre
l_{crit}	Critical length in Shear-lag theory
l_p	Projected length of a fibre
n_1-n_4	Number of kinks in a specific degree interval
n_f	Number of fibres crossing the rupture zone that take load at failure and break
n_p	Number of fibres crossing the rupture zone being pulled out since they do not carry any load due to bond breakage
P	Fibre perimeter, fibre circumference
r	Fibre radius
RBA	Relative bonded area of a sheet
RSS	Residual sum of squares
TMP	Thermomechanical pulp
V_f	Volume fraction of fibres
WRV	Water retention value
Z	Z-parameter

Z_c	Finite-span tensile strength of a strip without any bond breaks
β	Mean force applied along the fibre axis required to pull a fibre from a sheet
λ	Slenderness ratio
μ	Poisson's ratio.
ρ	Density
ρ_c	Density of cellulose
ρ_s	Apparent sheet density
σ_f	Ultimate axial stress
σ_T	Tensile strength of paper
σ_T^w	Tensile strength index
σ_{TC}	Tensile strength of composite
σ_{ZD}	Z-strength
σ_{ZS}^w	Zero-span tensile strength
τ	Uniform shear stress
τ_b	Shear strength between fibres
φ	Mean fibre strength